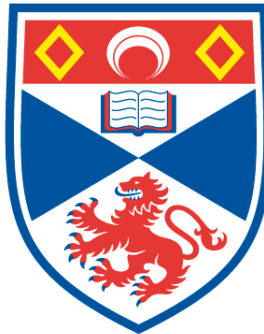


MT5999 ADVANCED PROJECT IN MATHEMATICS

Mathematical Modelling of Tumour-Induced Angiogenesis

Chiara VILLA

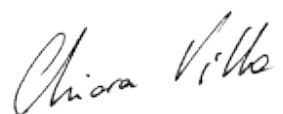
April 27, 2018



University of
St Andrews

Supervisor:
Professor M. A. J. CHAPLAIN

*I certify that this project report has been written by me, is a record of work carried out by me, and
is essentially different from work undertaken for any other purpose or assessment.*

A handwritten signature in black ink, appearing to read "Chiara Villo".

Abstract

Solid tumours are small due to oxygen limitation, but have the ability to stimulate angiogenesis, the formation of a new vascular network from pre-existing blood vessels. Thanks to this they can further expand and eventually metastasise. This work explores the mechanisms behind tumour-induced angiogenesis and the role that mathematical modelling has in the study of the process. The first part of this document is dedicated to the biological description of angiogenesis. This includes the steps of the process, the enzymes involved in it, the structure of the new vascular network and its consequences in tumour progression. Then three early continuum models of tumour-induced angiogenesis are presented and solved numerically. The first is a one-dimensional model (Chaplain & Stuart, 1993) and it sheds light on the role of migration and proliferation of endothelial cells in the formation of new sprouts. The first two-dimensional model of angiogenesis (Orme & Chaplain, 1997) highlights the role of chemotaxis in cell migration and that of haptotaxis in loop formation. Various anti-angiogenesis strategies are also simulated. The third model, focusing on cells at the sprout tips (Anderson & Chaplain, 1998), confirms the importance of haptotaxis in the successful completion of angiogenesis.

Contents

1	Introduction	1
2	The Biology of Angiogenesis	4
2.1	Blood vessels and the circulatory system	4
2.2	Angiogenesis	5
2.2.1	Embryogenesis	8
2.2.2	Wound healing	8
2.2.3	Tumour-induced angiogenesis	10
3	Mathematical models of angiogenesis	14
3.1	Overview of mathematical modelling	14
3.2	A simple 1D model of Tumour-Induced Angiogenesis	15
3.3	Two-dimensional models of Tumour-Induced Angiogenesis	20
3.3.1	Inclusion of haptotaxis and simulation of anti-angiogenesis strategies	20
3.3.2	Towards a discrete description of angiogenesis	26
4	Conclusion	33
A	Nondimensionalisation	37
B	Numerical simulations	39
B.1	Matlab code for solution to Chaplain&Stuart model	39
B.2	COMSOL	41

Chapter 1

Introduction

Mathematical biology is an interdisciplinary research field which combines tools and techniques in applied mathematics to study the mechanisms behind systems and processes in ecology, biology and medicine. It provides an alternative framework in which to test hypotheses and formulate new ones, with the potential to optimise time and cost of experimental procedures.

The formulation of mathematical models to study cancer origin and progression only started in the second half of the twentieth century and since then a wide portion of scientific literature has focused on this field [1]. Not only is cancer a fascinating topic, but due to the complexity of its nature we are still far from understanding how it works and how to cure it, leaving a lot of questions still unanswered. Moreover, the complex nature of cancer allows the use of a wide variety of mathematical tools in the construction and study of its models. Aside from the scientific interest, this field of study has a strong element of humanity motivating researchers, as cancer has a strong impact on people's lives – if not directly, then through family and friends. Every year over 8 million people are dying from cancer worldwide, a number only expected to increase over the coming years [2], making it important to study tumours from as many perspectives and fields as possible.

The mechanisms behind it make cancer one of the most evolutionary “smart” collection of diseases, able to adapt to harsh environments and avoid harmful processes. Cancer cells are able to proliferate uncontrollably, resist cellular death, as well as evade growth suppressors and immune attacks. In order not to starve, they can change their metabolism as well as induce the formation of new vasculature from pre-existing vessels to ensure sufficient blood supply. They can enter the bloodstream and form metastases, colonising other parts of the body. These and many other evolutionary advantages are collectively known as the hallmarks of cancer [2, Week 3: Ten Cellular Hallmarks of Cancer].

Angiogenesis is the formation of new vasculature from pre-existing blood vessels, one of the hallmarks of cancer. This process comes up in many different contexts, including embryogenesis and wound healing. However, the main focus of this paper will be on tumour-induced angiogenesis. Solid tumours starved of oxygen and nutrients induce the formation of new blood vessels to reinforce their blood supply, with which they can move from the avascular to the vascular stage of tumour progression and grow even further. Without angiogenesis, tumours would not be able to metastasise.

The process itself starts with the activation of endothelial cells on the parental vessel by chemical agents known as angiogenic factors or, in the case of tumour-induced angiogenesis, tumour angiogenesis factors (TAF). Then the activated endothelial cells proceed to degrade the basement membrane of the parental vessel and migrate towards the source of TAF, i.e. the tumour. The movement of cells up the

gradient of a chemical, here the TAF, is a mechanism known as chemotaxis. After initial movement, endothelial cells also start to proliferate, slowly constructing new vessels. The extracellular matrix also has a key role in the migration of cells, which go up the gradient of the matrix's components, a mechanism known as haptotaxis. The combination of these two processes leads to branching – a sprout splits in two – and anastomosis – nearby sprouts merge into one. These processes eventually lead to the formation of loops and a well structured vascular network in which blood can flow.

Even though these are the key steps of angiogenesis that will be considered in the models presented in this document, the angiogenic process and its activation are a lot more complex. The second chapter of this report is aimed at conferring the complexity of the mechanisms behind angiogenesis. Starting with a brief overview of blood vessel structure and the circulatory system, the chapter describes the role of angiogenic factors and heterotypic interactions in the main steps of angiogenesis. After a brief description of the process during embryogenesis and wound healing, details of tumour-induced angiogenesis will be presented, including how solid tumours trigger it, the consequences in tumour progression and the role of anti-angiogenesis strategies in therapy.

The notions presented in the second chapter could be described in greater detail [3], however only a few key concepts are necessary to understand the models described in the rest of this document. In fact, mathematical models are by definition a simplification of reality, aimed at gaining a deeper understanding of the system modelled. Oversimplification would result in the loss of realistic results, but the model still needs to be approachable either analytically or numerically to get some insight in the problem: the right balance is needed for the model to be valid. In the words of Helen Byrne, “*the models are only ever as good as the assumptions used to construct them and the data with which they are validated*” [1]. The models presented in chapter three have experimental observations, validated results of previous models or well known biological facts behind the assumptions used to construct them, as well as insights on comparison with experiments. It is fascinating to see how well such a simplification of reality can agree with real-life observations.

Mathematical models may be of different types to fit the nature of the system modelled. They may be stochastic or deterministic; the former ones include randomness properties, leading to different results with some probability, while the latter ones have no randomness and repeating simulations will lead to the same outcomes. We may have continuum models, in which continuous variables are involved, or discrete ones, where variables take values from a discrete state-space. In the context of mathematical biology and cellular systems, continuum deterministic models may describe the evolution in time of some continuous variable, such as cellular density, with the use of systems of ODEs or PDEs. The main three models discussed in this document will be of this kind, composed of systems of PDEs such as conservation equations involving chemotaxis and haptotaxis, together with appropriate boundary and initial conditions. There is however a widespread use of stochastic models to study tumour cells due to the random nature of their mutations and behaviours. Discrete stochastic models can describe the evolution of each cell individually, reason why they are also known as individual-based or agent-based models, as well as cellular automata models. In particular, discrete models taking the form of a random walk are quite popular. There is a third category of models, known as hybrid models, which combine the two approaches: cells may be modelled as individuals, using a cellular automata description, in a spatial domain in which other substances (e.g. oxygen, TAF) are described as a continuum. Moreover, from the microscopic description of an individual-based model, a corresponding macroscopic one can be derived in the form of a continuum model for the population of cells and viceversa. Such derivation usually results in a model which combines the strengths of both approaches. A brief description of the derivation of a discrete model from a continuum one can be found in section 3.3.2.

Chapter three will start with brief overview of the first models of angiogenesis, based on Helen Byrne's work [1]. This way, the main three models reproduced in this document will be placed in the bigger picture of academic literature. The rest of chapter three will focus on those three early models of tumour-induced angiogenesis. Assumptions and equations will be presented as in the corresponding papers. The equations have been solved numerically and the corresponding simulations will be presented, with observations on the results made in correspondence with the original papers.

The first paper considered describes a one-dimensional continuum model formulated by Chaplain and Stuart in 1993 [4], one of the first works focusing on angiogenesis. The study focuses on endothelial cells migration and proliferation, related to the concentration of TAF, therefore studying the role of chemotaxis. Section 3.3.1 is dedicated to the first two-dimensional continuum model of angiogenesis, proposed by Orme and Chaplain in 1997 [5]. This considers the role not only of chemotaxis but also haptotaxis in the completion of angiogenesis, by introducing fibronectin in the system of equations. A brief demonstration of how simple parameter manipulation may be used to simulate anti-angiogenesis strategies will also be given. The third model presented has been formulated by Anderson and Chaplain in 1998 [6] in order to study the role of chemotaxis and haptotaxis in the process, with a focus on the cells at the sprout tips. The main results of Anderson and Chaplain's investigation on different tumour geometries will also be mentioned, as well as their derivation of an agent-based model from the continuum description in the form of a biased random walk. Even though no simulations have been carried out for the resulting discrete model, the derivation and main results are important to mention due to their place in the academic literature of angiogenesis modelling. The intent of this chapter is not only to show how angiogenesis can be studied with mathematical models, but also how these models rely on each other and on experimental observations, resulting in an interdisciplinary and cooperative field of study.

The ideal target audience of this document involves applied mathematicians who are familiar with PDEs construction and are interested in the biological application discussed. In particular, this work has been carried out without assuming any prior knowledge of angiogenesis, therefore the key biological terms needed to understand the process and the mathematical models are explicitly defined and explained in chapter two. Since in the rest of that chapter lots of biological or medical terms are included which may not be familiar to the reader, a glossary has been added at the end of this document. The only pre-requisite to understanding this work is basic knowledge of the construction of a conservation equation, hence how different mechanisms may be translated into mathematical terms in a PDE. Overall, with this report, I hope to convey the importance of studying angiogenesis and the role mathematical modelling has in such investigation.

Chapter 2

The Biology of Angiogenesis

2.1 Blood vessels and the circulatory system

Blood vessels are tubular structures which carry blood throughout the body and they are part of the circulatory system. There are different types of blood vessels: arteries, arterioles, capillaries, venules and veins. They all vary in size, with the largest blood vessel having a diameter of 2cm - the aorta - while capillaries have a diameter as small as $5\mu\text{m}$ - smaller than a hair [7].

Capillaries are composed of a layer of endothelial cells: (ECs), covered by the basement membrane made up of connective tissue, usually including mural pericytes: and vascular smooth muscle cells:. Arteries and veins have a more laminated structure, made up of three main layers [7, Figure 2]. The outer layer, known as *tunica externa* or *adventina*, is quite thick and made out of connective tissue:. The *tunica media* – in the middle – is the thickest one made up of circularly arranged elastic fibers and smooth muscle cells, with arteries presenting more contractile tissue than veins. Finally, the inner layer is known as the *tunica intima*: it's the thinnest one, composed of a single layer of endothelium supported by a subendothelial layer. Veins also have valves in the lumen, to help the blood flow back to the heart [7].

Arteries carry oxygenated blood away from the heart with the help of the extra contractile tissue; through the arterioles, they are connected to the capillaries where the exchange of oxygen and carbon dioxide with the cells occurs. Nutrients are released to the tissue via the permeable endothelium of the blood vessels. Capillaries then deliver the blood, rich of waste products, from the cells to the veins – through the venules – and the veins carry it back to the heart. Because they are not as thick and strong as the arteries, the presence of valves ensures the blood flows in only one direction. Overall blood vessels form a network able to reach almost every cell in the body, which would be between 60.000 and 100.000 miles long if stretched out [8] – this would circle the globe more than twice! The circulatory network is vital for the organism, as the cells need to get oxygen and nutrients to function and survive.

Cells need oxygen as it breaks down sugar and hence produces energy during cellular respiration. In hypoxic conditions - i.e. in the absence of oxygen - cells are in danger of becoming necrotic: or, through the action of p53: [3, p.331], undergo apoptosis:. One possible defense mechanism for cells to survive is the switch to anaerobic respiration:, during which cells start to break down glucose as they normally would but end up with a smaller amount of energy and the accumulation of lactate:, causing acidosis:. A more advantageous process triggered by the cells in hypoxic conditions is angiogenesis.

2.2 Angiogenesis

Angiogenesis – from Greek *angeion* (vessels) and *genésis* (generation, production) – is a physiological process: through which new blood vessels are formed from pre-existing vasculature. It differs from neovascularisation and vasculogenesis as these terms refer to a *de novo*: formation of new blood vessels. It is a process which occurs in many different stages of the mammalian life, starting with embryogenesis:, through growth and development, to then have a key role in wound healing, implantation of the placenta and pathological process:es – such as tumorigenesis, diabetic retinopathy:, psoriasis:, rheumatoid arthritis:, duodenal ulcer:s and others. Despite these being very different contexts in which angiogenesis takes place, they all share the same key steps in the formation of new blood vessels from pre-existing vasculature. The steps described below refer to what is known as sprouting angiogenesis, rather than intussusceptive angiogenesis: or splitting angiogenesis [9]. Unless otherwise indicated, the information presented in this section has been taken from Weinberg's book *The biology of Cancer* [3], in particular from Chapter 13 of the book.

Angiogenic factors

The process starts thanks to the action of angiogenic growth factors, which activate the receptors of endothelial cells of which the existing blood vessels are made up. These factors can be produced or activated following different stimuli, some of which are described in the next sections in more specific angiogenic contexts. Table 1 below lists the most important angiogenic factors, specifying their main function [10,11]. It is important to stress however that signaling proteins involved in angiogenesis are much more than those listed and have many other functions and targets than those mentioned in the table.

Table 1: Angiogenic factors

Name	Full name	Main function
VEGF	Vascular endothelial growth factor	Stimulate endothelial cells (ECs) proliferation
PDGF	Platelet-derived growth factor	Induce smooth muscle recruit
aFGF	Acid fibroblast growth factor	Stimulate ECs proliferation and differentiation
bFGF	Basic fibroblast growth factor	Stimulate ECs proliferation
Ang1	Angiopoietin 1	Help stabilise vessels
Ang2	Angiopoietin 2	Destabilising blood vessels
TGF- α	Transforming growth factor alpha	Cell proliferation, differentiation and development
TGF- β	Transforming growth factor beta	extracellular matrix (ECM) production
MMP	Matric metalloproteinase	Degradate ECM proteins, keep vessel walls solid
Tsp-1	Trombospondin-1	Trigger ECs apoptosis (inhibitor)
IL-8	Interleukin 8	Promote cell migration
HGF	Hepatocyte growth factor	Stimulate mitosis and cell migration
uPA	Urokinase plasminogen activator	ECM degradation
Endostatin	Endostatin	Interfere with bFGF and VEGF (inhibitor)
Angiogenin	Angiogenin	Smooth muscle and ECs migration and proliferation, ECM and basement membrane degradation
Angiostatin	Angiostatin	Inhibition of ECs migration and proliferation, induction of apoptosis (inhibitor)

Once activated by the angiogenic factors, endothelial cells start to produce and release protease:s, enzymes which degrade the basement membrane of the vessel, allowing the cells to exit the vascular wall. Moreover these biological signals help recruit endothelial progenitor cells (EPCs:) produced in the bone-marrow, of which they also stimulate production, moving in the bloodstream. Once they have reached the angiogenic site, they can differentiate into endothelial cells thanks to the action of more angiogenic factors. These agents are also involved in many other steps of the process, like triggering mitosis: of various cell types bearing the corresponding receptor:s and therefore enhancing cellular proliferation, directing the new endothelial tubes where they are most needed and recruiting pericytes:.

Heterotypic interactions

The angiogenic factors produced often don't bind to the receptors of endothelial cells straight away, but are sequestered by the extracellular matrix (ECM:). When this happens, the angiogenic switch will not occur without either the action of other angiogenic factors or heterotypic interactions.

The term *heterotypic signalling* indicates the communication between different cell types, which is used by each of them to limit or boost proliferation of the surrounding cells. We have seen in section 2.1 how blood vessels are not just made up of endothelial cells, but also of other stromal cells: types which compose the connective tissue:. Stromal cells are mesenchymal cells: and make up a lot of the surrounding tissue, including the ECM, providing support for the parenchymal cells: (functional, not structural cells). The most common stromal cells are fibroblast:s, myofibroblast:s, endothelial cells, pericytes:, smooth muscle cells:, adipocytes:, macrophages: and lymphocytes:.

In normal tissue, heterotypic signalling depends on the exchange of mitogenic growth factor:s (HGF, TGF- α , PDGF), boosting proliferation, growth-inhibitory signals (TGF- β), limiting it, and trophic factors: (e.g. IGF-1, IGF-2). An example of heterotypic signalling is given by the role of myofibroblast:s to benefit nearby endothelial cells. These rely on the protein stromal cell-derived factor 1 (SCF-1) to recruit endothelial precursor cells (EPCs:) circulating in the bloodstream. Then they secrete VEGF which induces EPCs to differentiate into endothelial cells, promoting the formation of new vasculature. [3, p.579-581]

The main steps of angiogenesis

Angiogenic factors, with the help of heterotypic interactions as described above, activate those endothelial cells on existing blood vessels which present the corresponding receptor:s. Often the recruitment of inflammatory cells: is necessary to trigger the angiogenic switch. In fact macrophages:, stromal cells: which should find and eliminate infectious agents and abnormal cells as part of the immune system, actually secrete VEGF and IL-8 (vid Table 1), stimulating angiogenesis. This is the first of the main steps typical of any angiogenic process, which are summarised in figure 2.1. The angiogenic stimulus in the figure is described as in tumour-induced angiogenesis, more detail of which are given in section 2.2.3.

Then, as already stated, the activated endothelial cells produce and release protease:s, which proceed to degrade the basement membrane. Basement membrane degradation is stimulated by TAFs such as MMPs and ANG-2 (vid Table 1), also involving uPA Receptor. After this stage endothelial cells can migrate out of the vessel and proliferate. The recruitment of EPCs and differentiation into endothelial cells also increases the number of cells accumulating in this new sprout. Many angiogenic factors are involved in such process (e.g. VEGF, FGFs); of these, VEGF binds to the tyrosine kinase receptor:s on the surfaces of the endothelial cells, boosting proliferation and encouraging the construction of the

cylindrical walls of capillaries. These new vascular tubes grow towards areas with the highest localised concentration of angiogenic factors, making their way through the existing tissue layers, reaching those cells which required more vasculature in the first place. Tube formation and remodelling is stimulated and directed by various angiogenic factors, such as VEGF and FGFs, with destabilising angiogenic factors, such as ANG-2, also involved. Moreover, movement of endothelial cells is also determined by integrins:, receptors responsible for cell-to-matrix interactions. At this stage, the endothelial tubes lack structural stability and are therefore unable to resist the force of blood pressure. Then other angiogenic factors (e.g. angiopoietins, TGF β) recruit pericytes: and smooth muscle cells: – the mural cells composing the outer layer of capillaries – to build the outer walls of the new blood vessels and hence finalise their construction. [3, p.582-585]

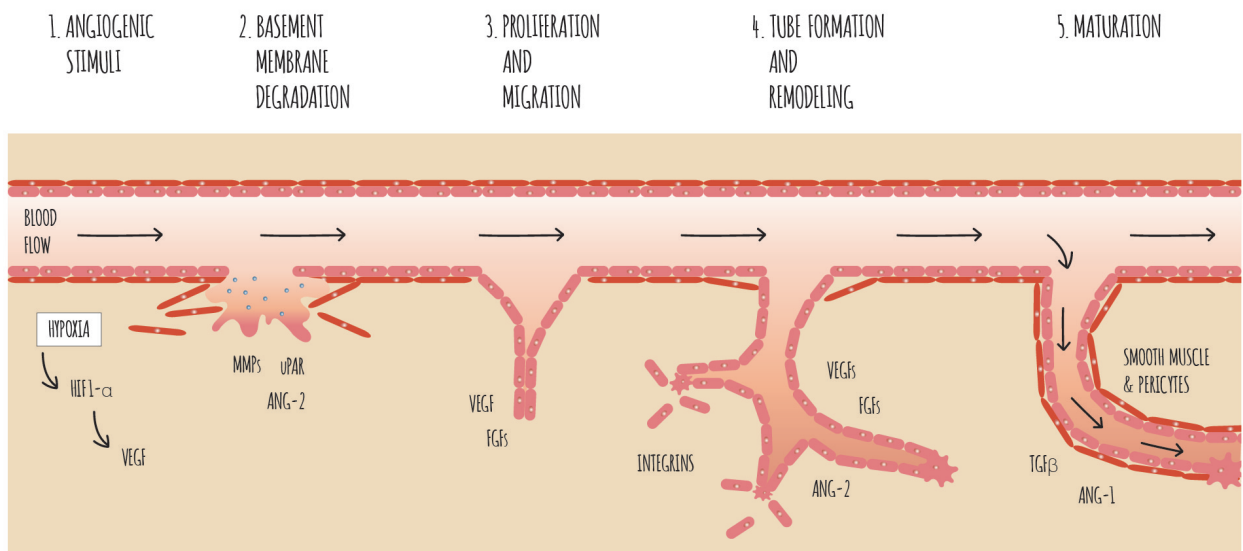


Figure 2.1: Main steps of angiogenesis, also mentioning the most important proteins of each step involved in tumour-induced angiogenesis. The angiogenic stimulus (1) comes from VEGF, produced by tumour cells after HIF1- α becomes functional in hypoxic conditions (vid section 2.2.3). Basement membrane degradation (2), proliferation and migration (3) of ECs, tube formation and remodelling (4) and maturation (5) are all stimulated and directed by angiogenic factors. Image by L. Govi, printed with permission from the artist

Once angiogenesis is completed, the new blood vessels become functional and start delivering oxygen and nutrients to the surrounding cells. However, they differ from the pre-existing vasculature in various ways. First of all, they have a diameter of up to three times greater than normal vessels, allowing more space in the bloodstream for cells to circulate in. Moreover the walls are ten times more permeable as the plasma membranes of adjacent endothelial cells are not in direct contact with each other, resulting in leaky vessels: blood plasma reaches surrounding cells directly, with an accumulation of fluid in spaces between parenchymal cells: [3, p.614]. Such structure also allows cells to enter the bloodstream easily. This has serious consequences, especially when the cells surrounding the new vessels are tumour cells.

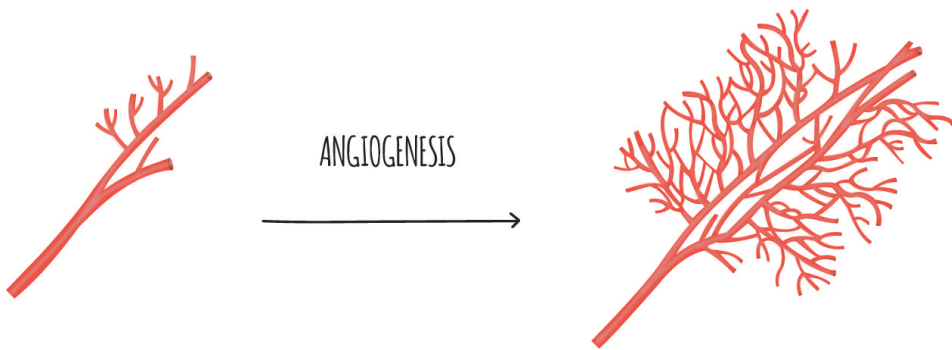


Figure 2.2: Blood vessels before and after angiogenesis: the network as expanded with sprouts splitting in two or merging with nearby ones, eventually forming loops in the network. Image by L. Govi, printed with permission from the artist.

2.2.1 Embryogenesis

The information presented in the following has been taken from a review of angiogenesis in embryonic development [12], in which the role of VEGF and angiopoietins are discussed in much greater detail.

The first angiogenic process in the life of an individual occurs during embryonic development. The circulatory system is the first organ to develop in the embryo with the first blood vessels forming through vasculogenesis, thanks to the differentiation of EPCs. The resulting primitive vascular network is then extended and modified via angiogenesis, both sprouting and intussusceptive. VEGF has a key role in this process, as well as Ang1 in recruiting pericytes and smooth muscle cells. The overall layout of the major blood vessels is determined by the genome of each individual, but local capillary networks are designed and constructed by the cells in the tissue. Hence the role of heterotypic interactions is key in determining the route of the local vascular network.

Interestingly, embryonic angiogenesis occurs in anticipation of the need for oxygen of the growing embryo, rather than in response to signals following the decrease of oxygen levels, determining the main difference between angiogenesis in this context and that of tumour growth.

2.2.2 Wound healing

The information presented in this subsection has been taken from Patrick Simon's work on skin wound healing, easily accessible on the Medscape website [13], as well as section 13.3 of *The biology of Cancer* [3, p.587-600].

After an injury, consisting of a superficial wound to the skin and underlying tissues, the body has a restorative response that leads to tissue regeneration. This happens in different stages which can be summarised in homeostasis, inflammation, proliferation and maturation. During the third phase, angiogenesis occurs.

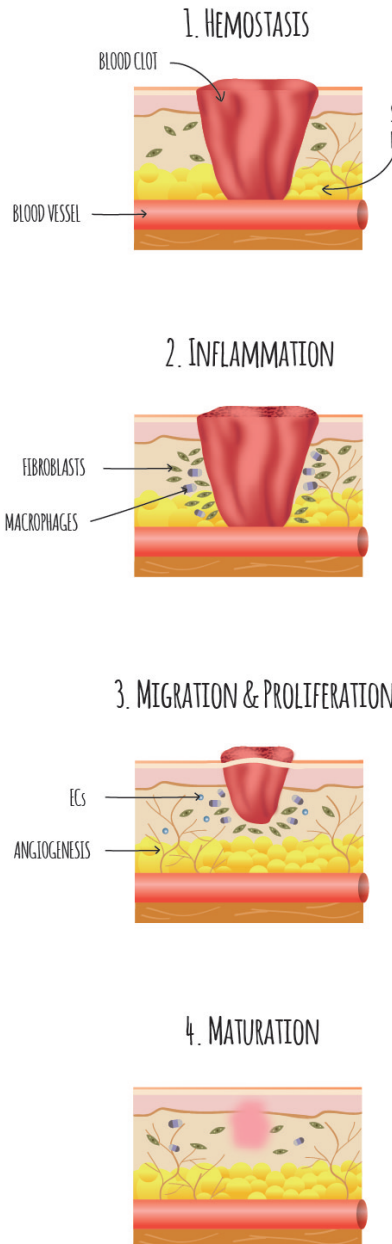


Figure 2.3: Stages of wound healing, with the main cells involved indicated. Angiogenesis occurring in stage 3. Image by L. Govi, printed with permission of the artist.

As soon as the injury takes place, homeostasis starts with the aggregation of blood platelets: which release cytokines:, chemokines;, hormones and later chemotactic and growth factors, including PDGF and TGF- β (vid Table 1). Initial vasoconstriction to limit blood loss is later followed by the release of vasoactive agents. These increase the permeability of blood vessels near the wound and therefore help fibrinogen: molecules reach the wound site – fibrin: is essential to wound healing as it constitutes the scaffold of blood clots. The angiogenic factors help recruit fibroblast:s, stimulate their proliferation (PDGF) and activation (TGF- β). Fibroblasts produce and release other angiogenic factors: FGFs increase endothelial cell proliferation and MMP degrade specific components of the ECM. Such components will then be remodelled at later times with the new cells and will activate other growth factors. These, together with FGFs, attract different cell types which will remove foreign matter and bacteria, releasing more FGFs and VEGF.

During homeostasis, chemokines: attract inflammatory cells:, like macrophages:, to the site. This is facilitated by the increased permeability of the vasculature. Within the many functions of macrophages are the elimination of bacteria and debris and secretion of collagenase:s and elastase:s. These break down injured tissue and release cytokines:, including PDGF which recruits and stimulates the proliferation of fibroblast:s and smooth muscle. Macrophages also releases angiogenic factors functioning as chemoattractants for endothelial cells and stimulating their proliferation.

The action of all these angiogenic factors – most importantly bFGF and VEGF – starts angiogenesis, also thanks to the recruitment of endothelial cells. This has been activated in response to low tissue oxygenation and is essential to providing a rich blood supply to the forming tissue. Angiogenesis follows the main steps described at the beginning of section 2.2, leading to a great blood flow in the wound site and increasing the amount of healing factors and structural cells. As the need for more blood decreases, the production of angiogenic factors will decrease so that the process of angiogenesis stops. Moreover Tsp-1 is a soluble inhibitor of growth factor receptors which also works towards inhibiting angiogenesis. The unfinished blood vessels present at this point will vanish by apoptosis.

In the formation of the new epithelial tissue, endothelial cells have reduced their adhesion to the ECM and increased motility through a temporary change in phenotype using endothelial-to-mesenchymal transition (ETM). This allows them to move more freely in the site and, once they have filled gaps in the tissue, they undergo mesenchymal-to-endothelial transition (MET) and reconstruct the epithelium. At this point stromal cells:, such as myofibroblast:, undergo a physical contraction to effectively close the wound. Collagen and cytokines: have an active role in the maturation phase, after which the new tissue resembles the pre-wound one. Overall it's clear that angiogenesis has a key role in wound healing and tissue regeneration.

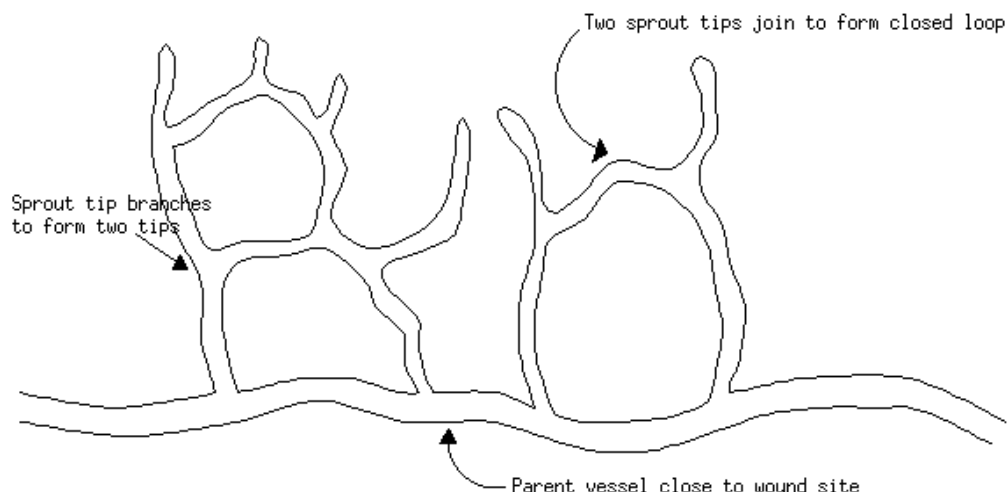


Figure 2.4: Structure of new blood vessels created via sprouting angiogenesis during wound healing. Image by Kake L Pugh, under CC BY-NC-SA licence (<https://creativecommons.org/licenses/by-nc-sa/4.0/>), retrieved from <http://www.earth.li/~kake/mathsmathbiol/angiogenesis.html>.

2.2.3 Tumour-induced angiogenesis

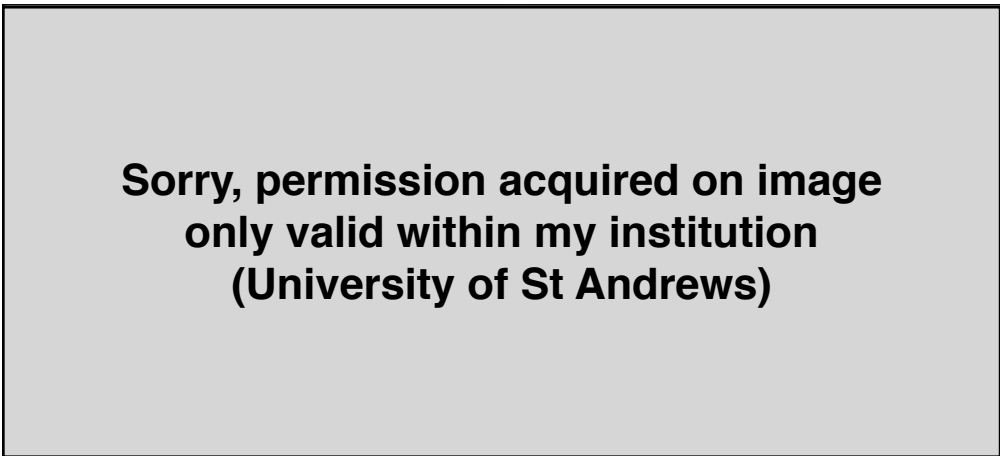
Wound healing angiogenesis and tumour-induced angiogenesis are very similar processes. Both are triggered by hypoxic conditions in the site, they have similar signalling pathways and both rely on heterotypic interactions, especially with inflammatory cells:

The tumours considered here are solid carcinomas (non-liquid cancers, e.g. not leukaemia). Hence the cells involved are neoplastic: epithelial cells and stromal cells: making up the connective tissue:. Carcinoma cells greatly depend on stromal support and stromal cells co-evolve with their neoplastic: neighbours.

Solid tumours grow from cancer cells' uncontrolled proliferation as multi-cellular spheroids. As they expand, the cells at the center don't have direct access to oxygen and nutrients coming from blood vessels and hence form a necrotic: core. In these hypoxic regions, cells lacking the adequate oxygen supply release angiogenic factors to stimulate capillary formation. Let's consider in detail how hypoxia triggers angiogenesis. [3, section 13.3,13.5]

Hypoxia-Inducible Factor 1 (HIF-1)

The HIF-1 is a transcription factor: activated by hypoxia. Figure 2.5 shows how in normoxic conditions, i.e. under normal oxygen supply, HIF-1 α is synthesised and hence made inactive. Its degradation involves many steps, one of which is its conversion to hydroxyproline:, carried out by an enzyme which depends on oxygen for its activity, known as pVHL [3, p.265-268]. Without oxygen, this conversion can't occur and the HIF-1 is not synthesised and its levels in the hypoxic area increase within minutes. Once functional, HIF-1 causes the expression of target genes related to angiogenic factors, increase the production of red blood cells, stimulates glycolysis: and glucose transport into the cell for alternative metabolism. Some of HIF-1 target genes are related to the production of angiogenic factors such as VEGF, PDGF and TGF- α (vid Table 1). As seen before, VEGF attracts and stimulates the proliferation of endothelial cells constructing the new blood vessels, while PDGF and TGF-1 target different cell types, including mesenchymal and endothelial cells. Then the main steps of angiogenesis lead to the formation of a new vascular network.



**Sorry, permission acquired on image
only valid within my institution
(University of St Andrews)**

Figure 2.5: Comparison of HIF-1 synthesis under normoxic conditions and VEGF transcription by HIF-1 under hypoxic conditions. Reprinted from Molecular Cancer Therapeutics, March 2012;11(3) [53848], N. Rahimi, *The Ubiquitin-Proteasome System Meets Angiogenesis*, with permission from AACR. Retrieved from <http://mct.aacrjournals.org/content/11/3/538>.

The process and the new vasculature

Just like during wound healing, hypoxic areas of tumours attract macrophages: through chemotaxis. Despite the fact that the role of macrophages is to block tumour development, these produce mitogenic growth factors and help remodelling the ECM, resulting to be important collaborators to tumour development. In fact mitogenic growth factors are pro-angiogenic factors and the ECM remodelling is a critical step for tumour invasion and metastases (more on this in the next subsection). Tumour-induced angiogenesis follows the same steps described in previous sections. The main tumour angiogenic factors released are VEGF, aFGF, bFGF and angiogenin (vid Table 1), inducing the degradation of the basement membrane by enzymes secreted by the cells with the corresponding receptors. Chemotactic signals help recruit endothelial cells and EPCs:, thanks to heterotypic interactions with stromal cells:

like myofibroblast:s and others previously mentioned, which then mature into endothelial cells aided by VEGF and start proliferating and assembling the new vasculature. [3, p.604-606]

It is interesting to notice that angiogenesis is not a binary state: different types of tumour cells are likely to show different abilities to attract endothelial cells and form new vasculature, which can be easily summarised in the notion of having greater or smaller angiogenic powers [3, p.626].

Once the new vascular network is formed, normal oxygenation is restored and the HIF-1 can be synthesised as in normoxic conditions, which ends the transcription and hence production of VEGF and other tumour angiogenesis factors. Many anti-angiogenic factors are also involved in arresting angiogenesis, including – just like in wound healing – thrombospondin-1 (TSP-1). The transcription of this gene is normally carried out by the p53: tumour-suppressor gene, in charge of apoptosis: [3, p.331]. In tumours, there is a loss of the p53 function as this gene is under-expressed. This results in a decrease in TSP-1 production and consequent promotion of tumour progression [3, p.623], however underlying mechanisms of p53 regulation and its role in tumour progressions still remain unclear and controversial. After a new capillary network has restored normoxia in the tumour site, TSP-1 transcription increases again and its action helps to stop angiogenesis. TSP-1 triggers apoptosis of endothelial cells which compose the newly formed or forming blood vessels, while it does not affect mature vessels.

Capillaries appear to form where they are most needed by parenchymal cells:, following the chemical gradients induced by hypoxia and depending not on genetic instructions but on localised heterotypic interactions, just like during embryogenesis. In this case, while vascular cells are endothelial cells, pericytes: and smooth muscle cells:; non-vascular types include neoplastic: and stromal cells:. The new vascular tubes formed have a blind ending and are called sprouts. As the network becomes more dense, loops are formed by fusion of sprouts – event known as anastomosis – just like during wound healing, as shown in figure 2.4. Moreover, marginal sprouts can break through the ECM and expand the vascular network. [3, p.607-614]

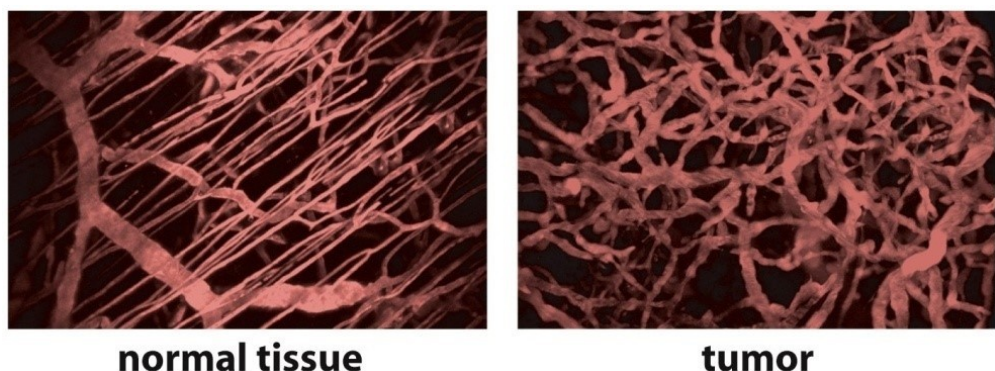


Figure 2.6: Comparison of local vascular network in normal tissue and tumours. Reprinted from DovePress, April 2017:5 [21-32], Forster JC, Harriss-Phillips WM, Douglass MJ and Bezak E, *A review of the development of tumor vasculature and its effects on the tumor microenvironment*, under CC BY-NC licence (<https://creativecommons.org/licenses/by-nc/3.0/>). Retrieved from <https://www.dovepress.com/a-review-of-the-development-of-tumor-vasculature-and-its-effects-on-the-peer-reviewed-fulltext-article-HP>.

The ECM consists of interstitial tissue:, collagen fiber:, fibronectin and other components. The way endothelial cells interact with the ECM: affects cell migration directly as their interaction with fibronectin improves cell adhesion to the matrix. In fact, not only endothelial cells synthesise and secrete fibronectin, but once this binds to the ECM the cells use it to attach themselves to the matrix via integrins: (receptor:s). Fibronectin therefore promotes migration of endothelial cells up its concentration gradient, a mechanism known as haptotaxis.

Consequences of angiogenesis in tumour progression

The new vasculature provides nutrient and oxygen supply to the tumour cells which risked necrosis before the angiogenic process. This means that angiogenesis provides the necessary resources for an avascular tumour, which generally reaches a diameter of at most 1-3mm, to grow in size. Moreover, since the new blood vessels are leaky and have a larger lumen – as already established – this allows tumour cells to enter the circulatory system and travel in it more easily. With angiogenesis the tumour reaches its avascular phase, after which invasion of normal tissue and intravasation: can occur, eventually leading to the possibility of metastasis [3, p.619]. While an avascular tumour, which is small and still local, can easily be removed or contained, if an individual presents metastatic sites at diagnosis, it might be too late to intervene efficiently [2, Week 4: Metastasis: the real killer].

Therapy

Despite angiogenesis being a very complicated process involving a wide network of factors and various cell types, its dependence on so many factors offers multiple targets of intervention. Below only a few highly targeted therapies are presented, most of which are still being studied in labs or are used in clinical trials:.

To prevent the angiogenic switch from occurring, angiogenesis inhibitors may be used to stop angiogenic factors from undergoing transcription and production. For example, drugs known as interferon- α and interferon- β suppress the synthesis of bFGF and IL-8. To reduce the impact of pro-angiogenic factors on tumour progression, monoclonal antibodies: may be used as they bind to the angiogenic factors and hence neutralise them. Therapy may also target their corresponding receptors on endothelial cells, so that even in the presence of factors like VEGF or PDGF cellular proliferation and other processes would not be activated.

To intervene after the angiogenic switch, angiogenesis inhibitors (angiotatin, endostatin) may also be used to block the growth of the new blood vessels. Such proteins are not toxic to the tissue as natives of the body, but are expensive and difficult to manufacture. Despite the fact that they have shown to be quite effective on the tumour vasculature and size, they are still on clinical trials. The endothelial cells recruited via angiogenesis have a normal stable genome, unlike tumour cells, and are therefore sensitive to cytotoxic: drugs, which can have drastic effects on the tumour-induced vasculature. Overall anti-angiogenic therapy has shown to have an important role in anti-tumour radiotherapy and some types of chemotherapy, possibly due to the high sensitivity of tumour-associated microvasculature, suggesting targeting micro-vessel cells rather than tumour cells as a strategy to improve anti-tumour therapies [3, p.626-634].

Anti-angiogenesis strategies can be very useful adjunctive therapies:, combined with radiotherapy or chemotherapy, as well as offering a good alternative to such treatments when too aggressive to the normal host tissue. Anti-angiogenesis may target vasculature of primary tumours to prevent metastasis as well as control the growth of metastases once they have already formed [5].

Chapter 3

Mathematical models of angiogenesis

3.1 Overview of mathematical modelling

The models described in this chapter have been chosen from key papers in the history of mathematical modelling of tumour-induced angiogenesis. A good overview of the first models for this process can be found in Helen Byrne's paper *Dissecting cancer through mathematics: from the cell to the animal model* [1]. In this article, the role and development of mathematical modelling of cancer is discussed, with sections following various stages of cancer from carcinogenesis, through avascular tumour growth, angiogenesis and vascular tumour growth, to finish with the role of models in the clinic.

It is clear that from the beginning of models of angiogenesis, mathematicians have based their assumptions on experimental information, also used for comparison with model results. In particular, Muthukkaruppan and coworkers' publication in 1982 [14] has had an important role in the validation of initial models. The first spatial model of tumour-induced angiogenesis was proposed by Balding and McElwain in 1985 [15], formulated to describe *in vivo* experimental tumour-induced vasculature. The model proposes a one-dimensional continuum description of capillary formation, similar to that formulated by Chaplain and Stuart in 1993 [4]. The model well reproduces how the vasculature migration towards the tumour speeds up as the tips get closer to the tumour itself, as well as the fact that vessel density has a peak right behind the peak of tip cells density. These and many other characteristics of angiogenesis have been reproduced in Chaplain and Stuart's model [4], as reported in section 3.2.

As previously mentioned, Orme and Chaplain's model in 1997 [5] was the first two-dimensional continuum description of the process, which allowed the introduction of haptotaxis and, as a consequence, branching and anastomosis. It was however clear that the weakness of models proposed up to that point laid in the impossibility to incorporate details of the vascular network morphology or distinguish between few large vessels and lots of small ones [1, 5]. With this in mind, it is clear why the derivation of a discrete model from a continuum one by Anderson and Chaplain in 1998 [6] is a key event in the timeline of this field of study.

The first probabilistic model of angiogenesis was developed by Stokes and Lauffenburger in 1991 [16], describing the movement of ECs by a probabilistic equation and the TAF concentration with a reaction-diffusion equation, hence a hybrid model. The results obtained shed light on the role of chemotaxis and random motion in the completion of the new vasculature and their agreement with experimental

results, according to Helen Byrne, highlighted the role of mathematical modelling to function as a bridge between *in vitro*: and *in vivo*: experiments [1]. Even though Anderson and Chaplain's model wasn't the first stochastic or individual-based model of tumour-induced angiogenesis [6, p.875], it started a new class of hybrid models. These model the movement of ECs at the sprout tips as a biased random walk, while other ECs simply follow their path, resulting in the formation of the new sprouts recalling a 'snail trail', name by which these models are known today.

Details on the morphology of the network then lead to inclusion of blood flow in the models, followed by chemotherapeutic agents in the blood stream. As details on the biochemistry behind angiogenesis have been discovered, new models focusing on signalling pathways and regulatory networks have been formulated, indeed focusing on TAFs and the corresponding receptors [1]. As more models are proposed, new challenges come from the clinic, as the need for personalised models to help patients increases, as well as the theoretical necessity to link different models and parameters. Clearly this field of study offers many open questions and directions of investigation, both from a mathematical and medical point of view.

3.2 A simple 1D model of Tumour-Induced Angiogenesis

The first model presented was proposed by Chaplain and Stuart in 1993 [4] and is one of the earliest models of tumour-induced angiogenesis. The model focuses on monitoring the progress of endothelial cells of the sprouts as they move towards the tumour across the ECM. The ECM itself is not modelled, but two conservation equations are derived to describe the evolution of the concentration of the TAF and the density of endothelial cells (ECs). The TAF is secreted by the tumour and diffuses in the tissue until it reaches the nearest endothelial cells: these then release enzymes which degrade the basement membrane, under stimulus of the TAF, after which migration toward the source of TAF and subsequent proliferation can occur. The focus of this model is on the last two steps described.

To simulate the model, a one-dimensional spatial domain is considered, where the tumour – which secretes TAF – is placed at the left end and the parental vessel – from which the endothelial cells depart – is placed at the right end. The distance between the two is assumed to be within the critical threshold distance of 2.5 mm, under which little or no vascularisation occurs.

The tumour angiogenesis factor has concentration $c(x, t)$, the conservation equation of which includes spatial diffusion, loss due to uptake by the endothelial cells and decay of the chemical. We assume linear Fickian diffusion, with diffusion coefficient D_c , and first-order kinetics governing the decay of TAF. The loss due to cells can be modelled as $f(c)g(n)$: the local rate of uptake by the cells $f(c)$ is assumed to be governed by Michaelis-Menten kinetics, as well as depending on cell density; we take $g(n) = n/n_0$ for simplicity. This gives a sink term in the conservation equation for the TAF concentration. Overall we have:

$$\frac{\partial c}{\partial t} = \underbrace{D_c \nabla^2 c}_{\text{diffusion}} - \underbrace{\frac{Q_c c n}{(K_m + c)n_0}}_{\text{sink term}} - \underbrace{\frac{dc}{dt}}_{\text{decay}}. \quad (3.1)$$

The initial condition is given by

$$c(x, 0) = c_0(x), \quad (3.2)$$

which needs to match the assumptions described above and, in particular, the boundary conditions. These come from the assumption that the TAF concentration is constant (c_b) at the tumour boundary and has decayed to zero at the parental vessel, positioned at $x = L$. Hence we have:

$$c(0, t) = c_b, \quad c(L, t) = 0. \quad (3.3)$$

The conservation equation for the endothelial cells density $n(x, t)$ has terms modelling cell migration, mitotic generation of new cells and cell loss due to the formation of buds. Cell migration is given by $\nabla \cdot \mathbf{J}$, where \mathbf{J} is the cell flux term made up of linear spatial diffusion $-D_n \nabla n$, with constant diffusion coefficient D_n , and chemotactic motion of cell up the gradient of the TAF $\chi_0 n \nabla c$, where χ_0 has been picked to be a constant for simplicity. We assume mitosis to be governed by logistic growth, with maximum mitotic rate r and loss due to anastomoses given by a second-order loss term. On the contrary, cell loss due to budding (formation of buds) is modelled by a first-order loss term, proportional to the proliferation rate constant k_p . Overall the equation is:

$$\frac{\partial n}{\partial t} = \underbrace{D_n \nabla^2 n}_{\text{diffusion}} - \underbrace{\chi_0 \nabla \cdot (n \nabla c)}_{\text{chemotaxis}} + \underbrace{rn \left(1 - \frac{n}{n_0}\right) G(c)}_{\text{mitosis}} - \underbrace{k_p n}_{\text{cell loss}}, \quad (3.4)$$

where the term $G(c)$ is defined by

$$G(c) = \begin{cases} 0 & \text{if } c \leq c^*, \\ \frac{c - c^*}{c_b} & \text{if } c > c^*. \end{cases} \quad (3.5)$$

This terms allows us to set a threshold concentration level of TAF c^* below which the endothelial cells do not proliferate. As a consequence, there is a clear distinction between the initial response of migration of endothelial cells under stimulus on TAF and the secondary response of proliferation.

Assuming that initially all endothelial cells are at the parental vessel, with constant cell density which does not change over time at the limbus, then the conservation equation (3.4) is complemented with the initial condition

$$n(x, 0) = \begin{cases} n_0 & \text{if } x = L, \\ 0 & \text{if } x < L, \end{cases} \quad (3.6)$$

as well as the Dirichlet boundary condition

$$n(L, t) = n_0. \quad (3.7)$$

At the other end of the spatial domain we set a zero Neumann boundary condition on $n(x, t)$, corresponding to having no flux of endothelial cells across the boundary of the solid tumour.

For the numerical simulations the nondimensionalised model has been used. It is simply presented in the next section, but the detailed steps of derivation can be found in Appendix A.

The nondimensionalised model

In order to simplify the model described by (3.1)-(3.7), we define new nondimensional variables by normalising the main ones using reference variables: c_b for the concentration of TAF, n_0 for the endothelial cell density, L for the spatial dimension and $\tau = L^2/D_c$ as reference time unit. Therefore the new variables are:

$$\tilde{c} = c/c_b, \quad \tilde{n} = n/n_0, \quad \tilde{x} = x/L, \quad \tilde{t} = t/\tau. \quad (3.8)$$

Substituting these in equations (3.1) and (3.4) and dropping the tildes, gives the following nondimensional equations, derived for a one-dimensional spatial domain:

$$\frac{\partial c}{\partial t} = \frac{\partial^2 c}{\partial x^2} - \frac{\alpha n c}{\gamma + c} - \lambda c, \quad (3.9)$$

$$\frac{\partial n}{\partial t} = D \frac{\partial^2 n}{\partial x^2} - \kappa \frac{\partial}{\partial x} \left(n \frac{\partial c}{\partial x} \right) + \mu n (1 - n) G(c) - \beta n, \quad (3.10)$$

where

$$G(c) = \begin{cases} 0 & \text{if } c \leq c^*, \\ c - c^* & \text{if } c > c^*, \end{cases} \quad (3.11)$$

and we have defined the new parameters

$$\alpha = \frac{L^2 Q}{D_c c_b}, \quad \gamma = \frac{K_m}{c_b}, \quad \lambda = \frac{L^2 d}{D_c}, \quad D = \frac{D_n}{D_C}, \quad \kappa = \frac{c_b \chi_0}{D_c}, \quad \mu = \frac{L^2 r}{D_c}, \quad \beta = \frac{L^2 k_p}{D_c}. \quad (3.12)$$

The initial conditions (3.2),(3.6) and boundary conditions previously defined become

$$c(x, 0) = c_0(x), \quad (3.13)$$

$$n(x, 0) = \begin{cases} 1 & \text{if } x = 1, \\ 0 & \text{if } x < 1, \end{cases} \quad (3.14)$$

$$c(0, t) = 1, \quad c(1, t) = 0, \quad (3.15)$$

$$n(1, t) = 1, \quad \left. \frac{\partial n}{\partial x} \right|_{x=0} = 0. \quad (3.16)$$

Numerical simulations and results

In this section the numerical solutions of the model are reproduced, following the work of Chaplain and Stuart. The TAF concentration and EC density have been plot over the domain at different times to monitor the progress of the angiogenic process, in figures 3.1 and 3.2.

The MATLAB code created to solve the system numerically, and hence plot the solution at different times, can be found in Appendix B.1. In the code, the Matlab inbuilt function *pdepe* has been used, as it automatically solves initial-boundary value problems for systems of parabolic or elliptic PDEs in one spatial dimension over time, using the method of lines.

The parameters used take values matching experimental data, either chosen by the authors of the paper by investigation or taken from earlier models [4]. We have $L = 2\text{mm}$, corresponding to the average distance between the tumour and the limbal vessels, while $\tau = 14\text{days}$, corresponding to the average duration of angiogenesis. However, for the numerical simulations, the nondimensional model has been considered. The nondimensional parameters corresponding to the results presented below are $\alpha = 10$, $\gamma = 1$, $\lambda = 1$, $D = 0.001$, $\kappa = 0.75$, $\eta = 100$, $c^* = 0.2$ and $\beta = 4$. Details on this can be found in the paper [4]. Moreover, the initial condition for the TAF concentration is taken to be $c_0(x) = \cos(\frac{1}{2}\pi x)$, which automatically satisfies the boundary conditions (3.15) and the assumed initial profile of $c(x)$.

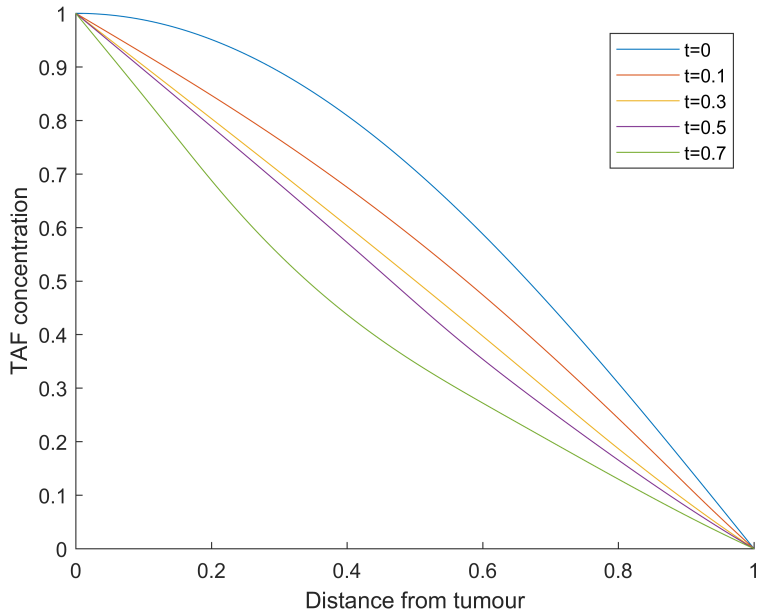


Figure 3.1: Numerical solution for the TAF concentration over the domain at different times.

First of all, it is important to remember that the model is only valid as the ECs are crossing the ECM. When they reach the tumour they will interact with it and, since the model is not aimed at investigating such dynamics, its main assumptions no longer hold. Therefore the solutions have been plotted and studied as long as $n(x, t)$ is small near $x = 0$. Such condition holds up to $t = 0.7$, which corresponds to a period of 11 days. It is clear from figure 3.1 that the TAF concentration decreases over time, as the ECs move towards the tumour and consume more of it. The overall profile of $c(x, t)$, however, doesn't change much over time, but can be easily replaced by a profile decaying linearly from the tumour to the vessel. Such an observation justifies assumptions in future models of a fixed linear profile of the TAF concentration, although in this case it may be due to the use of Dirichlet BCs. The ECs profile, shown in figure 3.2, moves towards the tumour over time, as expected since the ECs move up the gradient of TAF concentration, which has a maximum at the left boundary of the domain. It is easy to see from the plot that at initial times the ECs are mainly migrating towards the tumour and only start to proliferate later, when they are closer to the TAF source and hence have a higher

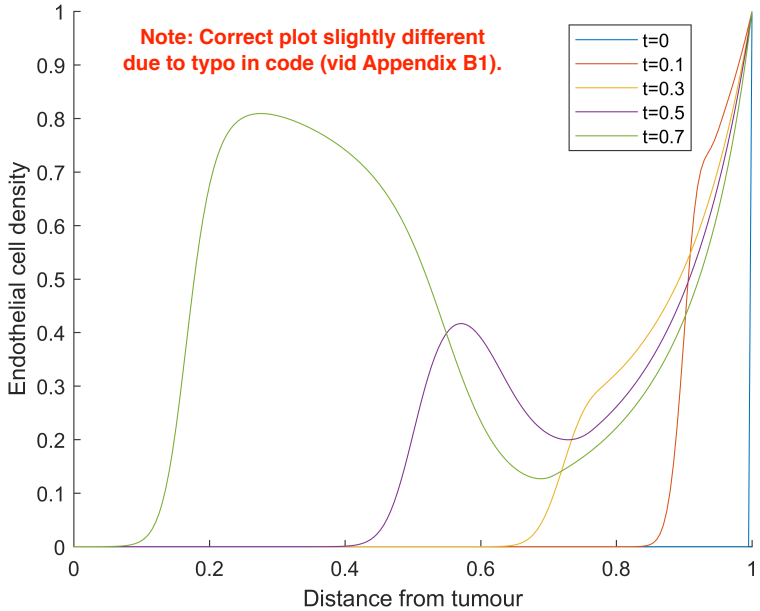


Figure 3.2: Numerical solution for the endothelial cell density over the domain at different times.

concentration of TAF available. Looking at the profile of $n(x, t)$ at different times, it is also clear that proliferation mainly occurs in the region right behind the sprout tips. In fact in that region, at later times, $n(x, t)$ has a local maximum.

Further results obtained with this model by Chaplain and Stuart [4] highlight the separation between a first phase of migration of ECs and a second one of proliferation. Setting $\kappa = 0$, hence removing chemotaxis and migration from the model, results in very little cell response to the TAF, indicating migration as a key first step in angiogenesis. Similarly, eliminating EC proliferation by setting $\eta = 0$ results in the reach of a steady state – after about 3.5 days – in which ECs are still far from the tumour, despite chemotaxis. Clearly both migration and successive cell proliferation are needed for angiogenesis to occur. On the contrary, diffusion seems to have negligible effects on the solution, which remained almost the same setting $D = 0$. Finally, removal of the tumour – modelled by setting zero flux instead of Dirichlet BCs for $c(x, t)$ at $x = 0$ – causes the decay of the TAF concentration to zero and regression of sprouts and vessels, completed after 14 days.

The results obtained from the model seem to agree well with what has been observed experimentally and with previous models, validating the model itself. Unlike previous models, this allows direct tracking of ECs progression towards the tumour, as well as its regression when the tumour is removed. Despite these improvements, the model could still be extended to include the sprout tip density or to study the role of the ECM in the process. The 1D model, which at each point of the one-dimensional domain studies the averaged EC density in the corresponding line of the two-dimensional domain, does not allow direct tracking of processes such as anastomosis or budding. The extension of the model to a 2D spatial domain would therefore lead to the inclusion of such structural processes in the study.

3.3 Two-dimensional models of Tumour-Induced Angiogenesis

3.3.1 Inclusion of haptotaxis and simulation of anti-angiogenesis strategies

Orme and Chaplain presented the first two-dimensional continuum model of tumour-induced angiogenesis [5] which captured features such as capillary sprouts growth, branching and anastomoses. The initial proposed model includes two conservation equations for the concentration of the TAF and the ECs density respectively, similarly to the model presented above, as well as a conservation equation for the density of an adhesive chemical, such as fibronectin. As described in section 2.2.3, this comprises the ECM and promotes migration of endothelial cells up the concentration gradient, a process known as haptotaxis. Fibronectin, component of the ECM functioning as the adhesive chemical in haptotaxis, is assumed to be produced by the ECs. The new vascular network needs a well defined structure to allow good blood circulation and hence the successful completion of angiogenesis, a matter in which haptotaxis – as resulting from this model – seems to have a key role. Moreover, the model allows us to simulate various anti-angiogenesis strategies by simple parameter manipulation, as presented in the *numerical simulations and results* section.

The two-dimensional domain is the square x - y domain $\mathcal{D} = [0, L] \times [0, L]$, where the tumour is placed at the lower boundary $y = 0$ and the parent vessel at the top boundary $y = L$. Let $n(\mathbf{x}, t)$ denote the ECs density, $c(\mathbf{x}, t)$ the concentration of TAF and $p(\mathbf{x}, t)$ the density of fibronectin – the adhesive chemical – at position $\mathbf{x} = (x, y)$ and time t . The flux term in the PDE for the evolution of $n(\mathbf{x}, t)$ includes spatial diffusion, with coefficient D_1 , chemotaxis – the ECs move up the gradient of TAF – and haptotaxis – the ECs move up the gradient of the adhesive chemical – with constant chemotactic coefficient κ and haptotactic coefficient χ respectively. Proliferation is modelled by logistic growth with proliferation rate μ and carrying capacity n_0 . Cell loss is assumed to be linear at rate β and it models drug-induced cell death, unlike in the 1D model in which it models budding in equation (3.4). Both $p(\mathbf{x}, t)$ and $c(\mathbf{x}, t)$ undergo Fickian diffusion, with coefficients D_1 and D_2 , and decay linearly at rates λ_1 and λ_2 respectively. They also exhibit similar uptake by the cells, at rates s_1 and s_2 . In addition, the adhesive chemical is produced by the cells at maximum rate α with threshold level B . Overall we have:

$$\frac{\partial n}{\partial t} = \underbrace{D_1 \nabla^2 n}_{\text{diffusion}} - \underbrace{\chi \nabla \cdot (n \nabla p)}_{\text{haptotaxis}} - \underbrace{\kappa \nabla \cdot (n \nabla c)}_{\text{chemotaxis}} + \underbrace{\mu n \left(1 - \frac{n}{n_0}\right)}_{\text{mitosis}} - \underbrace{\beta n}_{\text{cell loss}}, \quad (3.17)$$

$$\frac{\partial p}{\partial t} = \underbrace{D_2 \nabla^2 p}_{\text{diffusion}} + \underbrace{\frac{\alpha np}{B + p}}_{\text{production and saturation}} - \underbrace{s_1 np}_{\text{uptake by cells}} - \underbrace{\lambda_1 p}_{\text{decay}}, \quad (3.18)$$

$$\frac{\partial c}{\partial t} = \underbrace{D_3 \nabla^2 c}_{\text{diffusion}} - \underbrace{s_2 nc}_{\text{uptake by cells}} - \underbrace{\lambda_2 c}_{\text{decay}}. \quad (3.19)$$

Due to the large amount of parameters, the analysis of the results would be more difficult, especially regarding the biological interpretation. Hence, even after nondimensionalisation, the TAF profile will be assumed to have reached its steady state, resulting in a model with only two PDEs. This simplification is considered to be reasonable due to the much faster diffusion of TAF in comparison to that

of the ECs and it does not interfere with the aim of the model, which focuses on the role of haptotaxis.

The nondimensionalised model

Given a reference EC density n_0 , a typical density of the adhesive chemical p_0 and the initial TAF concentration c_0 , the nondimensional model is derived by substitution of the variables:

$$\tilde{n} = n/n_0, \quad \tilde{p} = p/p_0, \quad \tilde{c} = c/c_b, \quad \tilde{x} = x/L, \quad \tilde{y} = y/L, \quad \tilde{t} = t/\tau, \quad (3.20)$$

where, similarly to the previous model, L gives the size of the domain and τ is the time unit of reference. After substitution, the newly defined nondimensional parameters are:

$$\begin{aligned} \tilde{\chi} &= \frac{p_0\tau\chi}{L^2}, & \tilde{\kappa} &= \frac{c_0\tau\kappa}{L^2}, & \tilde{\mu} &= \mu\tau, & \tilde{\beta} &= \beta\tau, & \tilde{D}_i &= \frac{D_i\tau}{L^2} \quad (i = 1, 2, 3), \\ \tilde{\alpha} &= \frac{\alpha n_0\tau}{p_0}, & \tilde{\tau} &= \frac{1}{s_1 n_0}, & \tilde{s}_2 &= \frac{s_2}{s_1}, & \tilde{B} &= \frac{B}{p_0}, & \tilde{\lambda}_i &= \lambda_i\tau \quad (i = 1, 2). \end{aligned}$$

The new simplified model will then be nondimensional and will model the TAF concentration by assuming it to linearly decrease from the tumour to the parental vessel, as suggested by Chaplain and Stuart [4]. Hence we have $c(x, y) = 1 - y$. Dropping the tildas, the model is:

$$\frac{\partial n}{\partial t} = D_1 \left(\frac{\partial^2 n}{\partial x^2} + \frac{\partial^2 n}{\partial y^2} \right) - \chi \left[\frac{\partial n}{\partial x} \frac{\partial p}{\partial x} + \frac{\partial n}{\partial y} \frac{\partial p}{\partial y} + n \left(\frac{\partial^2 p}{\partial x^2} + \frac{\partial^2 p}{\partial y^2} \right) \right] - \kappa \frac{\partial n}{\partial y} + \mu n (1 - n) - \beta n, \quad (3.21)$$

$$\frac{\partial p}{\partial t} = D_2 \left(\frac{\partial^2 p}{\partial x^2} + \frac{\partial^2 p}{\partial y^2} \right) + \frac{\alpha np}{B + p} - np - \lambda_1 p, \quad (3.22)$$

with appropriate initial and boundary conditions for $n(\mathbf{x}, t)$ and $p(\mathbf{x}, t)$. Details on the steps of derivation are similar to those in Appendix A. We assume an initial distribution of ECs such that there are four initial capillary sprouts, which will also define the boundary conditions along the top boundary of the domain. As fibronectin is produced by the ECs, it has similar initial conditions. Overall at $t = 0$ we have

$$n(x, y, 0) = \begin{cases} 1 & \text{if } (x, y) \in [0.11, 0.17] \cup [0.35, 0.41] \cup [0.59, 0.65] \cup [0.83, 0.89] \times [0.9, 1] \\ 0 & \text{otherwise} \end{cases}, \quad (3.23)$$

$$p(x, y, 0) = \frac{1}{2}n(x, y, 0). \quad (3.24)$$

Then the boundary conditions for the EC density at the top boundary are given as defined in equation (3.23), while everywhere else both $n(\mathbf{x}, t)$ and $p(\mathbf{x}, t)$ satisfy zero flux boundary conditions:

$$n(x, y = 1, t) = 1 \quad \text{if } x \in [0.11, 0.17] \cup [0.35, 0.41] \cup [0.59, 0.65] \cup [0.83, 0.89], \quad (3.25)$$

$$\frac{\partial n}{\partial x} = 0 \quad \text{at } y = 1 \quad \text{if } x \notin [0.11, 0.17] \cup [0.35, 0.41] \cup [0.59, 0.65] \cup [0.83, 0.89], \quad (3.26)$$

$$\frac{\partial n}{\partial x} = \frac{\partial p}{\partial x} = 0 \quad \text{at } y = 0, \quad (3.27)$$

$$\frac{\partial n}{\partial y} = \frac{\partial p}{\partial y} = 0 \quad \text{at } x = 0 \quad \wedge \quad x = 1. \quad (3.28)$$

Numerical simulations and results

The numerical solutions have been carried out with COMSOL. This makes use of the finite element method, with Lagrange quadratic elements as basis functions and the backward Euler time-stepping method for integration of the equations (Appendix B.2). The parameters used take values $D_1 = 0.0025$, $\chi = 0.5$, $\kappa = 0.65$, $\mu = 5$, $\beta = 0$, $D_2 = 0.5$, $\alpha = 5$, $B = 0.001$ and $\lambda_1 = 0.5$. The domain used for the numerical simulations is a square of unit side length, where the parental vessel is at the top boundary at $y = 1$, while a line of tumour cells is placed at the lower boundary at $y = 0$.

The endothelial cell density $n(x, y, t)$ has been plot at times $t = 0.8$ and $t = 1.2$ in figures 3.3 and 3.4 respectively. The effect of chemotaxis is evident from both images as the endothelial cells clearly migrate from the four initial sprouts towards the tumour. It is also easy to notice that the endothelial cells density, and hence cell proliferation, has a maximum right behind the sprout tips, just like what has been observed from Chaplain and Stuart's one-dimensional model in figure 3.2. The addition of fibronectin in this model allows us to visualise the effects of haptotaxis as well. In figure 3.3, the ECs density starts to have a T-shaped structure, indicating the beginning of branching at the sprout tips to form secondary sprouts. As this continues it will eventually form tip-to-tip anastomosis, indeed shown in figure 3.4 where we can see that these secondary branches merge once they have reached each other. Note also that the sprouts now have a well-defined structure, allowing the blood to circulate in the new vasculature: haptotaxis has a key role in this, as has been shown by Anderson and Chaplain [6], details of which are presented in the next section. Another interesting feature to notice from figure 3.4 is that even after branching and anastomosis the ECs density is higher at the front of the migrating new vessels: this is known as the *brush-border effect*, as first described by Muthukkaruppan *et al.* [14], and it is due to the increase in sprout branching as the vasculature gets closer to the tumour.

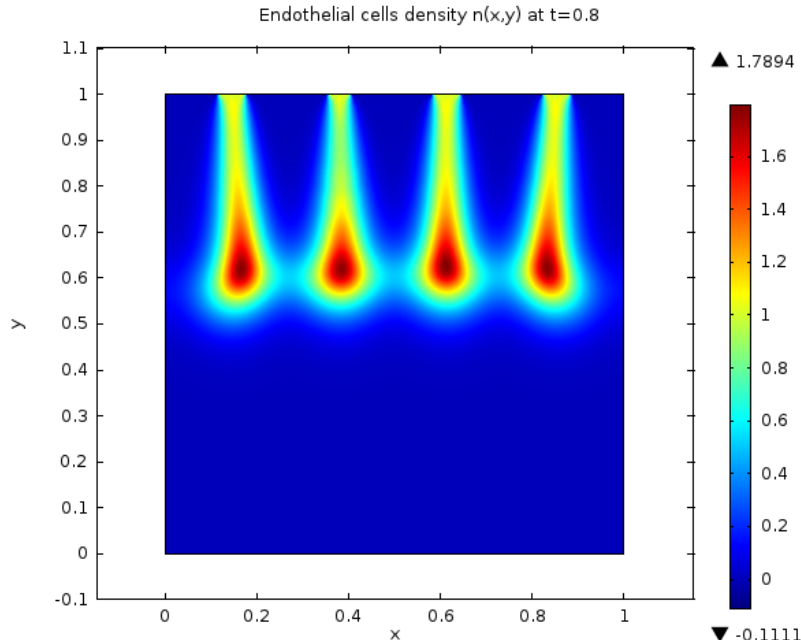


Figure 3.3: Numerical solution for the ECs density $n(x, y)$ at $t = 0.8$, showing sprout tips branching.

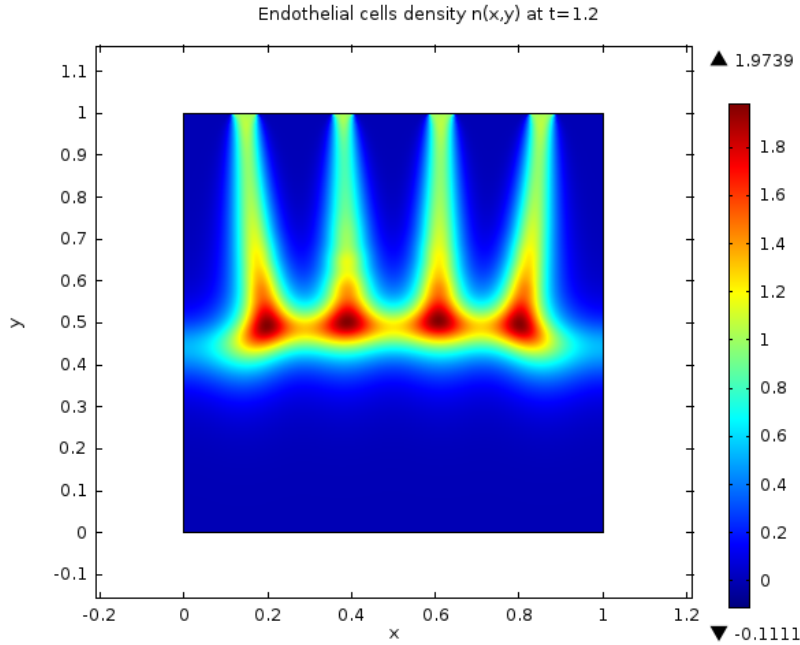


Figure 3.4: Numerical solution for the ECs density $n(x, y)$ at $t = 1.2$, showing tip-to-tip anastomosis.

As previously mentioned, simple parameter manipulation allows us to investigate possible anti-angiogenesis therapies. Orme and Chaplain have considered four possible strategies [5], each of which is here presented and plotted at times $t = 0.1$ and $t = 1.2$, to show over-time development of the vasculature under treatment. The absence of a specified parameter value for the timescale τ in the original paper [5] limits the inferences that can be made by comparing numerical results with real-life observations. However the acknowledgment of possible treatment investigation in this new two-dimensional setting marked the importance of this study.

The first anti-angiogenesis strategy considered is *cytotoxic targeting of ECs*, during which endothelial cells are killed. This can be simulated by setting $\beta = 50$ in the model. With this treatment the risk is that the parental vessel may also be affected, but there seem to be strategies to avoid it, for example by inducing ECs apoptosis only during the proliferative phase of the cell cycle: this way only proliferating cells are targeted, leaving pre-existing vessels unaffected. The numerical simulations are shown in figure 3.5, where it is clear that there is complete regression of the sprouts from the beginning of the therapy and further vessel formation is prevented.

The next strategy simulated is based on the *inhibition of cell mitosis*, therefore prevents ECs proliferation. The interruption of cell mitosis may be induced by some chemical agent, for example by angiostatin. This can be modelled by setting $\mu = 0$. The numerical results in figure 3.6 show how sprouts stop growing at early stages of treatment (3.6a). Despite ECs migration continues, the lack of proliferation prevents functional vessels from forming as no loops arise in the vasculature (3.6b). The last two strategies target cell migration rather than proliferation. First we consider *anti-chemotaxis* therapy, which relies on the obstruction of TAF receptors on ECs preventing them from responding to the presence of a TAF gradient. This can be simulated by setting $\kappa = 0$. From the plots in figure 3.7 it is clear that angiogenesis is prevented as vessels do not grow and the only change in ECs density is due to haptotaxis and cell proliferation, all confined in a region close to the parental vessel.

Finally *anti-haptotaxis* strategies, which rely on blocking fibronectin receptors, can be modelled by setting $\chi = 0$. Despite new vessels form at early times (3.8a), the absence of haptotaxis prevents distinct vessels to develop and at later times (3.8b) it seems that ECs have spread across the domain without forming a well-defined structure. This would not allow proper blood circulation, defeating the purpose of angiogenesis. The study of this anti-angiogenic strategy also highlights the importance of haptotaxis.

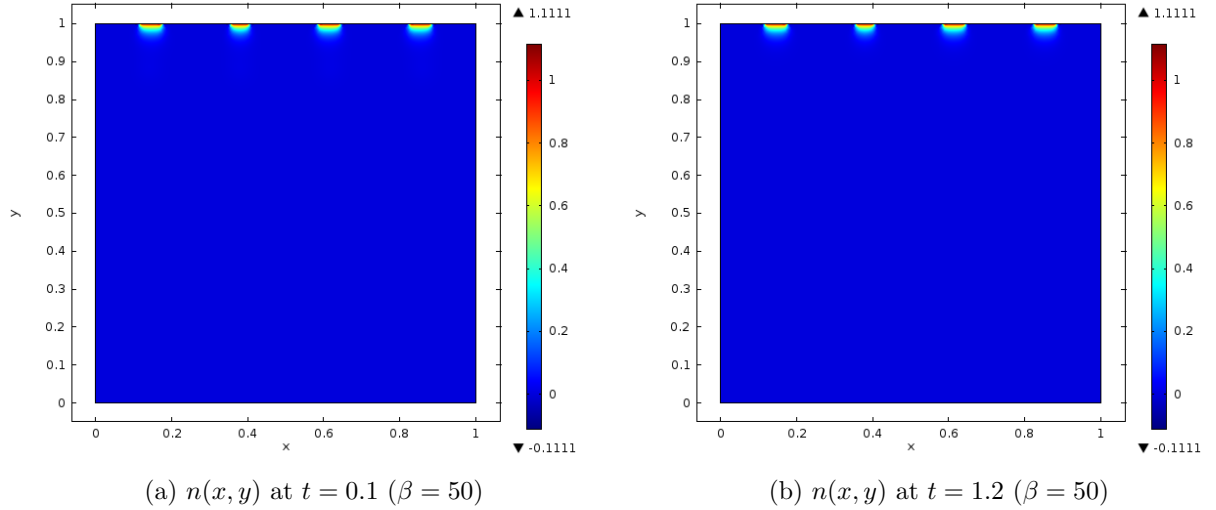


Figure 3.5: Simulation of ECs density during cytotoxic therapy ($\beta = 50$) at (a) $t = 0.1$ and (b) $t = 1.2$.

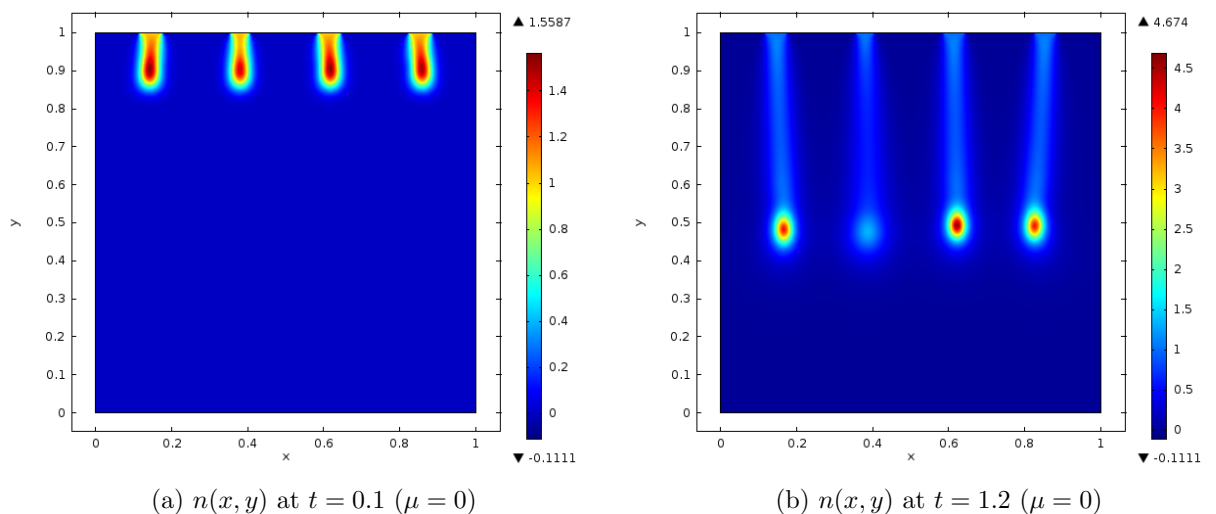


Figure 3.6: Simulation of ECs density during therapy through inhibition of cell mitosis ($\mu = 0$) at (a) $t = 0.1$ and (b) $t = 1.2$.

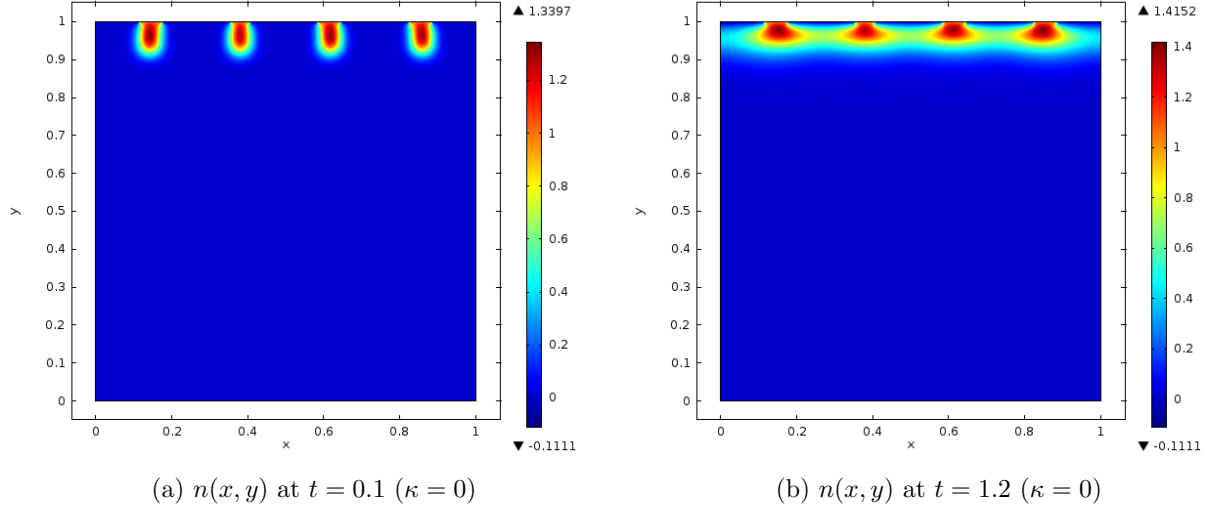


Figure 3.7: Simulation of ECs density during anti-chemotaxis therapy ($\kappa = 0$) at (a) $t = 0.1$ and (b) $t = 1.2$.

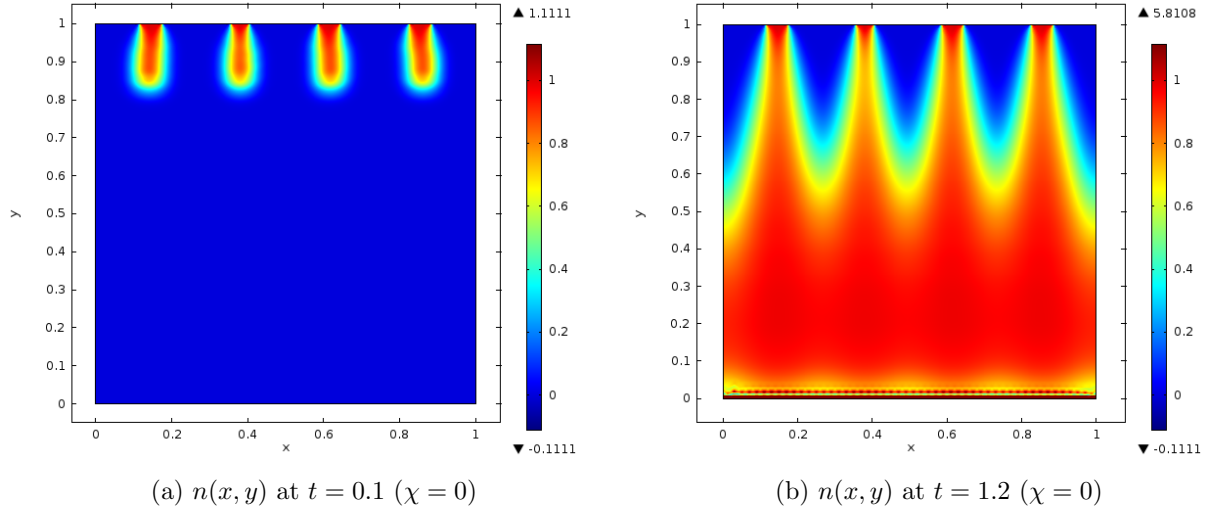


Figure 3.8: Simulation of ECs density during anti-haptotaxis therapy ($\chi = 0$) at (a) $t = 0.1$ and (b) $t = 1.2$.

Overall the model introduces a two-dimensional domain while highlighting the role of haptotaxis in angiogenesis. While chemotaxis plays a key role in the outgrowth of vessels directed towards the tumour, haptotaxis ensures the formation of a well-defined structure in which blood can circulate. Both are essential to successful completion of angiogenesis, as well as ECs proliferation. Despite all observations that can be made from this model, including remarks on branching and anastomosis, it is not possible to visualise the morphology of the new vascular network, as the dependent variable $n(x, y, t)$ simply models the density of ECs across the domain. To study the paths followed by the ECs and therefore the structure of the new sprouts an agent-based model is necessary. Interesting remarks on this can be found in the paper presented in the next section.

3.3.2 Towards a discrete description of angiogenesis

In 1998 Anderson and Chaplain presented both a continuum model and the corresponding discrete probabilistic model, in the form of a random walk [6]. Up to this point both continuum and discrete, deterministic and stochastic models for tumour-induced angiogenesis had been proposed and this paper has the advantage of presenting strengths of each approach. In this report, only the continuum model is described and simulated, but the discrete biased random walk can be derived from a discretised form of the PDEs of the first model [6, section 4]. The main results of the discrete model are briefly presented after the *numerical simulations and results* section. While the discrete model includes proliferation of ECs to visualise the structure of the new vascular network, the continuum one focuses on the ECs at the sprout tips, which do not undergo proliferation, so such mechanism is not included in the PDE for the ECs density. The continuum model is aimed at investigating the role of chemotaxis and haptotaxis in the migration of ECs, which is why the focus is on the sprout tips cells. Two tumour-geometries can be considered, to allow for comparison with previous models and experimental results. In particular Anderson and Chaplain have considered experiments presented by Sholley *et al.* [17] and Muthukkaruppan *et al.* [14], both studying neovascularisation *in vivo*: in mouse cornea, either induced by inflammation [17] or due to implanted tumour fragments [14].

Let $n(x, y, t)$ be the EC density, $c(x, y, t)$ the TAF concentration and $f(x, y, t)$ the concentration of fibronectin. Then the model will be described by a system of three PDEs. As already mentioned, the focus is on the sprout tips cells, so no proliferation term is included in (3.29), giving an equation without a reaction term. The flux term is then composed of random motility modelled by Fickian diffusion with coefficient D_n , haptotaxis with constant haptotactic coefficient $\rho_0 > 0$ and chemotaxis with the chemotactic function given by the receptor-kinetic law $\chi(c) = \chi_0 k_1 / (k_1 + c)$. Here both the chemotactic coefficient χ_0 and k_1 are positive constants and the chosen chemotactic function is based on the assumption that the chemotactic sensibility of ECs decreases as the TAF concentration increases. This is a more realistic assumption than considering it to be constant as in previous models. Fibronectin is produced and secreted by ECs at rate ω , after which it becomes bound to the ECM, hence does not diffuse. ECs then bind to it as they migrate towards the tumour with an uptake rate μ . The TAF, after secretion by tumour cells and diffusion in the ECM, reaches a steady state at the end of the first phase of angiogenesis. Such steady state will give the initial condition of the TAF for the model. Then the TAF concentration changes in time only due to uptake and binding by the ECs at rate λ . Overall the system of PDEs is given by:

$$\frac{\partial n}{\partial t} = \underbrace{D_n \nabla^2 n}_{\text{random motility}} - \underbrace{\nabla \cdot \left(\frac{\chi_0 k_1}{k_1 + c} n \nabla c \right)}_{\text{chemotaxis}} - \underbrace{\rho_0 \nabla \cdot (n \nabla f)}_{\text{haptotaxis}}, \quad (3.29)$$

$$\frac{\partial f}{\partial t} = \underbrace{\omega n}_{\text{production}} - \underbrace{\mu n f}_{\text{uptake}}, \quad (3.30)$$

$$\frac{\partial c}{\partial t} = - \underbrace{\lambda n c}_{\text{uptake}}. \quad (3.31)$$

These are coupled with appropriate ICs, depending on the setting considered, and no-flux boundary conditions. For $\underline{\zeta}$ the outward unit vector normal to the boundary, the BCs are of the form

$$\underline{\zeta} \cdot (-D_n \nabla n + n(\chi(c) \nabla c + \rho_0 \nabla f)) = 0. \quad (3.32)$$

The spatial domain considered is a square domain of size L , representing a square of corneal tissue, where the parent vessel is located at one edge, at $x = 0$, and the tumour at the opposite edge, at $x = L$.

The nondimensionalised model

For simplicity, the model in (3.29)-(3.32) has been nondimensionalised by rescaling the dependent and independent variables using some reference values and defining new parameters, similarly to the work done in Appendix A. Such reference values are n_0 , c_0 , and f_0 for the EC density, TAF and fibronectin concentration respectively. We then have L for space and $\tau = L^2/D_c$ for time, where D_c is the TAF diffusion coefficient introduced when deriving the initial conditions for the model in equation (3.37). Then setting $\tilde{c} = c/c_0$, $\tilde{f} = f/f_0$, $\tilde{n} = n/n_0$ and $\tilde{t} = t/\tau$, substituting them in the system of PDEs, rearranging and dropping the tildes gives the nondimensional system:

$$\frac{\partial n}{\partial t} = D \nabla^2 n - \nabla \cdot \left(\frac{\chi}{1 + \alpha c} n \nabla c \right) - \rho \nabla \cdot (n \nabla f), \quad (3.33)$$

$$\frac{\partial f}{\partial t} = \beta n - \gamma n f, \quad (3.34)$$

$$\frac{\partial c}{\partial t} = -\eta n c, \quad (3.35)$$

where

$$D = \frac{D_n}{D_c}, \quad \chi = \frac{\chi_0 c_0}{D_c}, \quad \alpha = \frac{c_0}{k_1}, \quad \rho = \frac{\rho_0 f_0}{D_c}, \quad \beta = \frac{\omega L^2 n_0}{f_0 D_c}, \quad \gamma = \frac{\mu L^2 n_0}{D_c}, \quad \eta = \frac{\lambda L^2 n_0}{D_c}.$$

Then the no-flux BCs are given by

$$\underline{\zeta} \cdot \left(-D \nabla n + n \left(\frac{\chi}{1 + \alpha c} \nabla c + \rho \nabla f \right) \right) = 0. \quad (3.36)$$

The ICs for the model simulations are as follows. As previously mentioned, the IC of the TAF concentration is considered after the first phase of angiogenesis, during which the TAF secreted by tumour cells diffuses into the ECM until it reaches the parent vessel. Considering natural decay of TAF as well, the initial profile is given by the steady state of the reaction-diffusion equation:

$$\frac{\partial c}{\partial t} = D_c \nabla^2 c - \theta c, \quad (3.37)$$

where D_c is the TAF diffusion coefficient and θ is the natural decay rate. Such steady state solution depends on the geometry of the domain: here we will only consider one setting, but Anderson and Chaplain have considered different ones [6].

We consider a row of tumour cells placed at the edge of the domain, at $x = 1$. Then an approximation to the steady state TAF concentration is given by

$$c(x, y, 0) = \exp\left(-\frac{(1-x)^2}{\epsilon_1}\right), \quad (x, y) \in [0, 1] \times [0, 1], \quad (3.38)$$

for ϵ_1 a positive constant. The other setting considered in Anderson and Chaplain's paper [6] is an approximately circular tumour centred at $(1, 0.5)$ of (nondimensional) radius of 0.1. This allows for comparison with results of *in vivo* experiments by Muthukkaruppan *et al* [14]. Then an approximation to the steady state TAF concentration is given by

$$c(x, y, 0) = \begin{cases} 1, & 0 \leq r \leq 0.1, \\ \frac{(\nu-r)^2}{\nu-0.1}, & 0.1 \leq r \leq 1, \end{cases} \quad (3.39)$$

where ν is a positive constant and $r = \sqrt{(x-1)^2 + (y-0.5)^2}$ is the distance from the center of the circular tumour. Even though the numerical simulations for this setting are not reproduced in this document, the key observations on the geometry of the domain resulting from such investigation are reported in the *numerical simulations and results* section below.

Aside from pre-existing fibronectin across the ECM, great amounts of laminin – another adhesive substance in the ECM – are found initially near the parental vessel. Moreover, as ECs' initial response to TAF stimuli is that of degrading the basement membrane of the parental vessel and therefore making it more permeable, this allows plasma fibronectin to leak out of the vessel and become bound to the ECM with high initial concentration around the vessel itself. Overall this leads to the initial concentration of fibronectin

$$f(x, y, 0) = k \exp\left(-\frac{x^2}{\epsilon_2}\right), \quad (x, y) \in [0, 1] \times [0, 1], \quad (3.40)$$

for positive constants $k < 1$ and ϵ_2 .

The migration of ECs only starts after the TAF has reached the parental vessel and the ECs have regrouped in a few clusters. Therefore for the IC for the EC density we consider three clusters, from which sprouts will form. This is given at the parental vessel edge of the domain at $x = 0$ in the form of three discrete peaks. For the numerical simulations presented in the next section, the following initial condition – which differs from the paper's one [6, p. 868] – has been used:

$$n(x, y, 0) = \exp\left(-\frac{x^2}{\epsilon_3}\right) \sin(6\pi(y - 0.08)), \quad \text{with } \epsilon_3 = 0.001. \quad (3.41)$$

Numerical simulations and results

The numerical simulations presented below have been computed with COMSOL, in a similar way to those in section 3.3.1 (vid Appendix B.2 for details). The parameter values used for the simulations are $D = 0.00035$, $\chi = 0.38$, $\alpha = 0.6$, $\rho = 0.34$, $\beta = 0.05$, $\gamma = 0.1$ and $\eta = 0.1$, together with $\epsilon_1 = \epsilon_2 = 0.45$, $\epsilon_3 = 0.001$ and $k = 0.75$ for the initial conditions. The parameters used to rescale space and time are the lengthscale $L = 2\text{mm}$, following the choice made in the first model presented, and the timescale $\tau = 1.5$ days.

The domain chosen is then a square with side of unit length with the parental vessel and three initial sprouts at the left boundary and a line of tumour cells at the right boundary. Since the model focuses on tip cells, there will be no proliferation. Because of this and the absence of cellular death, as well as the presence of zero flux boundary conditions, the total number of cells is conserved. We therefore focus on the migration of the tip cells and the shapes of the clusters. In figure 3.9 the ECs density has been plot at different times. Initially the clusters move towards the tumour along parallel routes, yet with lateral migration conferring them a crescent-like shape (3.9a). Once the tip cells from the clusters reach one another, anastomosis occurs (3.9b) and from there the ECs move towards the line of tumour cells as a continuous band (3.9c), with migration slowing down as this band gets closer to the tumour (3.9d). Figure 3.9d also show the previously described brush-border effect.

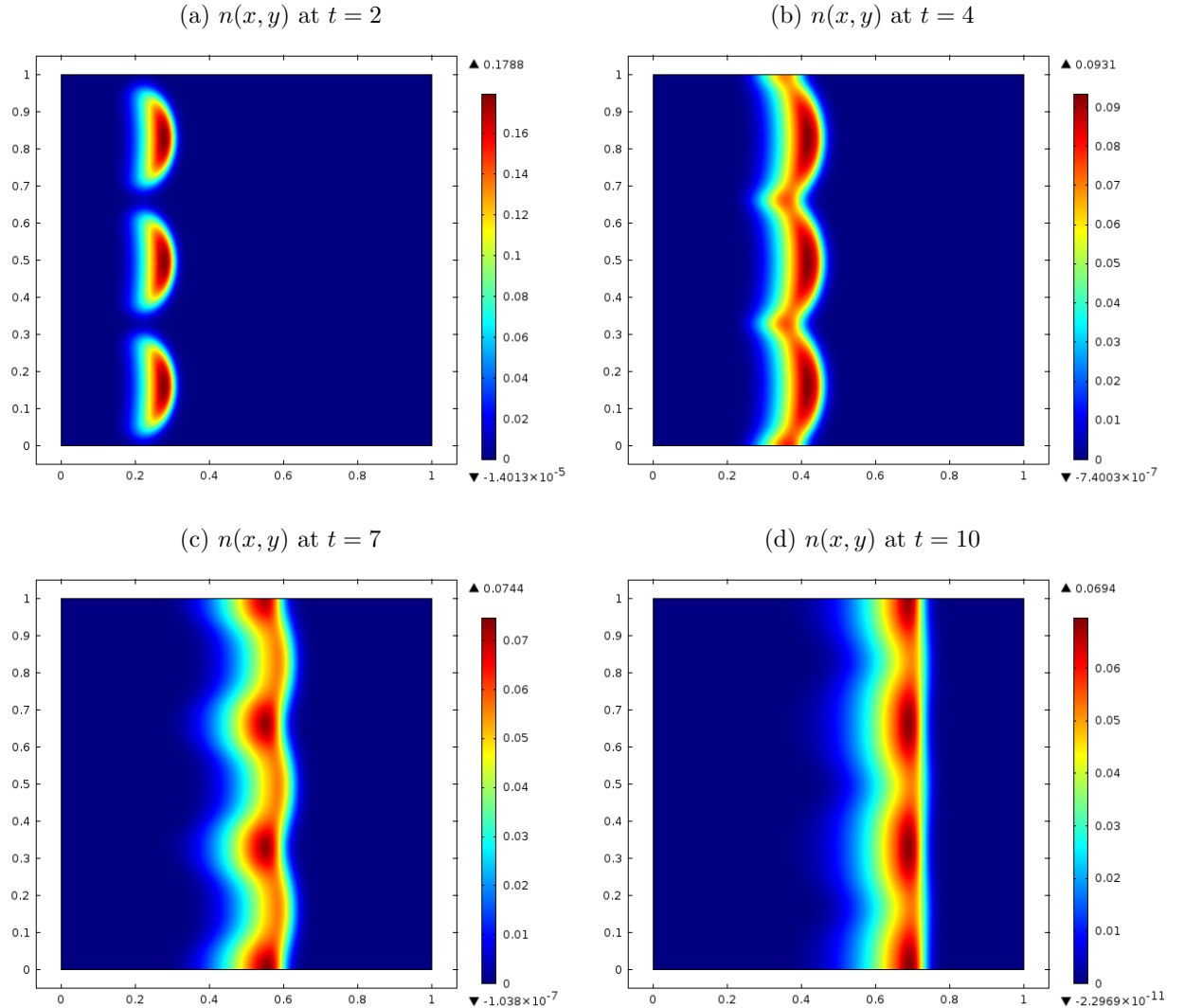


Figure 3.9: Plots of the endothelial cells density $n(x, y, t)$ at sprout tips given by Anderson and Chaplain's model including haptotaxis ($\rho = 0.34$) at various times.

As the ECs initially migrate towards the tumour, there is an uptake of fibronectin by the cells, which results in a gradient of fibronectin density in the direction perpendicular to that of cell migration. Due to haptotaxis, cells then start to move in such direction, clearly justifying the motion observed. Since in equations (3.29) and (3.33) chemotaxis has been modelled following the receptor-kinetic law, chemotactic sensitivity of ECs decreases as they get closer to the TAF source, resulting in fact in slower migration at later times. In particular, for α chosen large enough, the ECs may never reach the tumour [6]. This may explain the experimental results obtained by Sholley *et al.*, who demonstrated that initial vascular sprouts may form also in the absence of cell proliferation, resulting in a small network which never reaches the tumour [17].

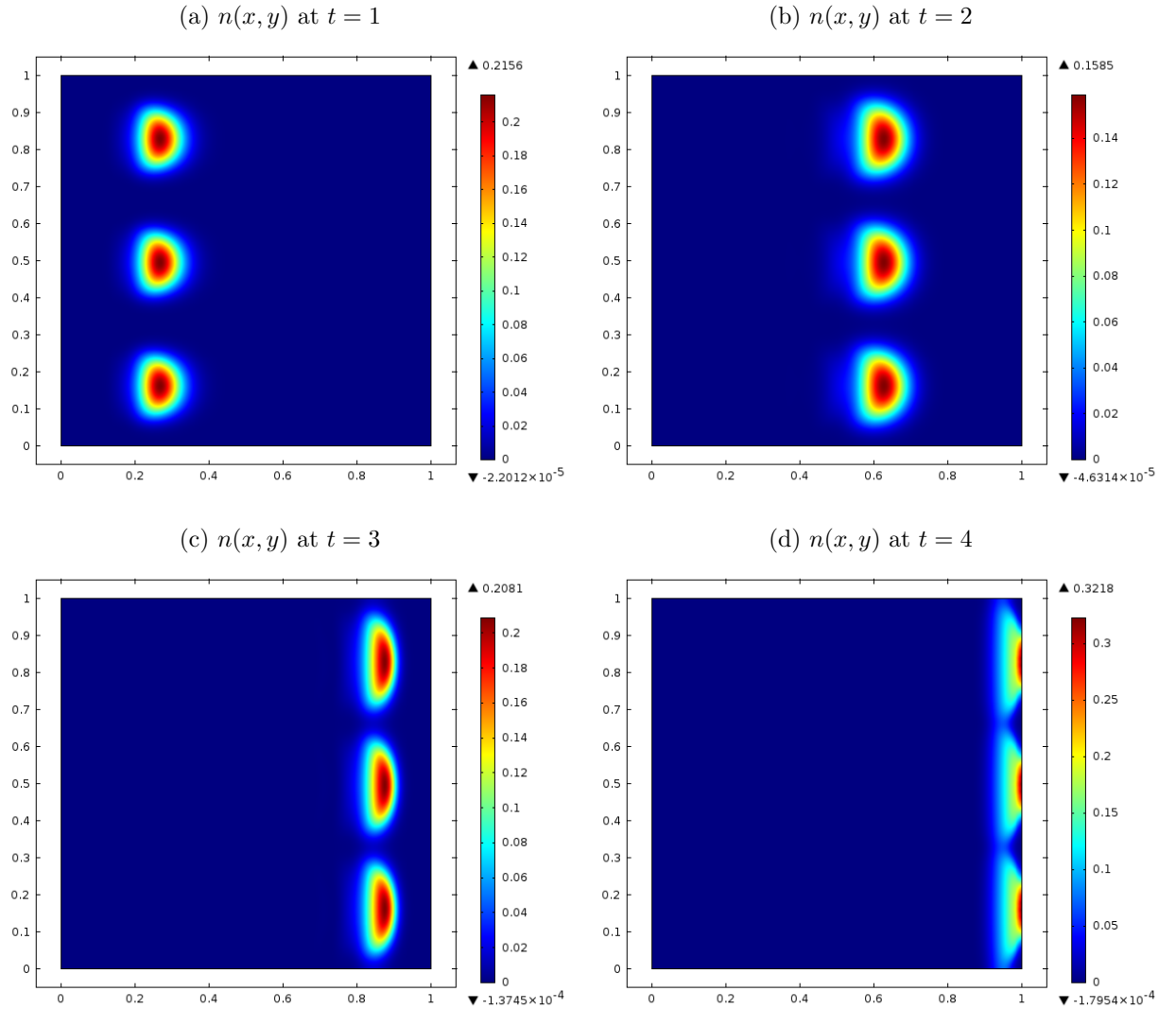


Figure 3.10: Plots of the endothelial cells density $n(x, y, t)$ at sprout tips given by Anderson and Chaplain's model without haptotaxis ($\rho = 0$) at various times.

By setting $\rho = 0$, we can study the model without haptotaxis to better understand its role on the movement of tip cells, or to simulate anti-haptotaxis therapy as done by Orme and Chaplain [5]. The plots of the numerical simulations for this case can be found in figure 3.10. Despite some lateral migration due to random movement, the clusters maintain a more spherical shape and travel towards the tumour parallel to each other. They reach the tumour a lot quicker than in the case with haptotaxis, as can easily be seen by comparing figures 3.9b and 3.10d. Clearly without haptotaxis no anastomosis has occurred and in the absence of loops in the new vascular network the blood can't flow in it. This matches the results inferred from figure 3.8 in the previous model. Investigation of network development at later times is not possible in this case with the model considered, as at $t = 4$ the tip cells reach the tumour and start interacting with it, so some assumptions no longer hold.

As previously mentioned, Anderson and Chaplain have also investigated the setting in which instead of having a row of tumour cells we consider a spherical tumour centered in the middle of the right-hand boundary, resulting in a TAF distribution given by equation (3.39). The numerical simulations show that, in this spherical geometry, the two lateral clusters of ECs initially move towards the central cluster as they go up the TAF gradient, until they merge into one big cluster [6, Figure 7]. The authors also noticed that at later times the ECs migrate towards the parental vessel and laterally: this clearly shows the importance of the geometry of the domain, as well as the role of the combination of TAF and fibronectin gradients.

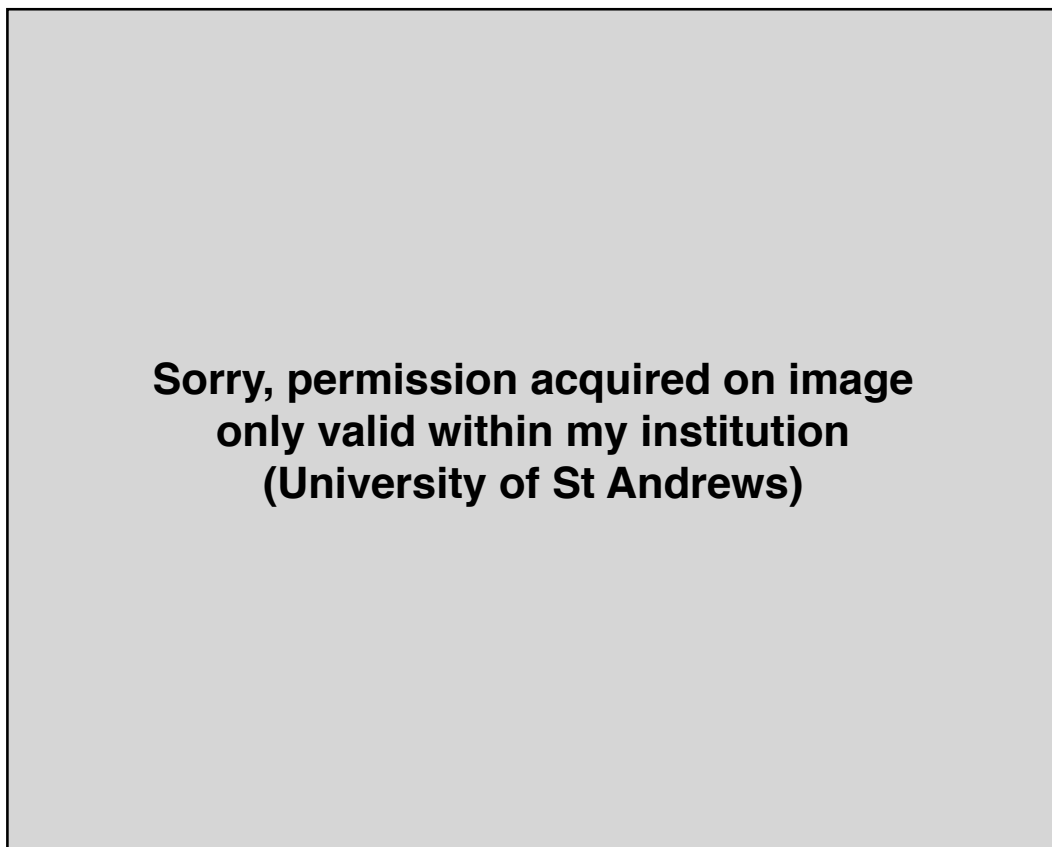
It is clear from this work that mathematical modelling has the flexibility to reproduce both *in vitro*: and *in vivo*: experiments, providing an alternative or complementary tool to investigate the mechanisms behind angiogenesis. In fact the domain chosen for the first set of numerical investigations may simulate the formation of vasculature in a square petri dish with a line of ECs along one side of the dish and a line of tumour cells along the opposite side. On the other hand, the settings described in the previous paragraph allow for comparison with *in vivo* experiments carried out by Muthukkaruppan *et al.* in 1982, when they monitored angiogenesis by implanting a small fragment of a solid tumour in the cornea of a mouse, close to the limbal vessel of the eye [14]. Drawings of the experimental results can be found in figure 3.11, clearly showing the angiogenic process and the brush-border effect.

Main results of the discrete model

As already mentioned, the discrete model was derived by discretising the PDEs of the continuum model, using the Euler finite difference approximation, resulting in probabilities of movement in the stochastic model strongly linked to the phenomenological rules of the deterministic one [6, p. 875-886]. The inclusion of proliferation allows tracking of ECs pathways and visualisation of network structure, as can be seen during experiments (e.g. figure 3.11). The results of the discrete model confirm those presented so far, with the advantage of allowing both qualitative and quantitative comparison with *in vivo* experiments. In the absence of haptotaxis, i.e. $\rho = 0$, the ECs undergo little lateral motion, progressing towards the tumour almost linearly. There is minimal branching and no anastomosis. With a circular TAF initial distribution, the ECs move towards the center of the domain – where the tumour is placed – but anastomosis does not occur. Results of the model with haptotaxis show a well spread network, with branching and lateral movement of tip cells, as well as anastomosis and a clear brush-border effect. In a circular setting, anastomosis occurs and, even though migration is slower, the overall vasculature formed is sufficient for blood to flow in it. Moreover, the absence of proliferation prevents the completion of angiogenesis.

Anderson and Chaplain have also looked at model results with proliferation only starting after 48 hours and occurring only in the region right behind the sprout tips. Such restrictions follow experimental results – stating that initial vasculature formation occurs even without proliferation [17] – as well as results from previous models [4]. The network resulting from these simulations reaches the tumour faster than in the previous cases.

Overall, the discrete model confirms the importance of haptotaxis in the formation of a well defined and realistic vascular network structure. This further highlights the role of cell-to-matrix interactions in the successful completion of angiogenesis. Moreover, the discrete model sheds light on how the geometry of the domain and the interplay of TAF and fibronectin gradients influence the final structure of the vascular network.



**Sorry, permission acquired on image
only valid within my institution
(University of St Andrews)**

Figure 3.11: Sequence of vascular response seen in mice cornea due to tumour fragment implantation. Drawings made every two days under stereomicroscope from experiments of Muthukkaruppan *et al.* [14]. Branching, anastomosis and brush border effect clearly visible after 10 days (e) and vascular stage of the tumour reached after 12 days (f). Reprinted from JNCI, September 1982;69(3) [699-708], V. R. Muthukkaruppan, L. Kubai and R. Auerbach, *Tumor-induced neovascularization in the mouse eye*, with permission from Oxford University Press. Retrieved from <https://doi.org/10.1093/jnci/69.3.699>.

Chapter 4

Conclusion

Angiogenesis is a very important process in the life of an individual, for example during embryogenesis and wound healing, but also has a key role in tumour progression. Therefore it may be necessary to promote angiogenesis in some contexts, but it is certainly vital that we study the process and how to stop it for those whose life is taken over by cancer. It is clear that a small solid avascular tumour is contained and not too harmful, but as it starves of nutrients and starts to become necrotic, it can trigger angiogenesis, creating a new vascular network from pre-existing blood vessels. The successful completion of this process will ensure a new blood supply for the tumour, which will then have reached its vascular phase and grow even further. Due to the leaky and wide structure of these new vessels, it will then be easier for tumour cells to intravasate and metastasise, at which point it may be too late to intervene.

From chapter 2, it is clear that angiogenesis is a very complex process which involves many angiogenic factors and depends on many molecular and heterotypic interactions. This makes it harder to capture all mechanisms involved in its progression and completion, but it also provides more opportunities for intervention, leading to a great potential for anti-angiogenesis therapies either on their own or combined with chemotherapy or radiotherapy. In fact, containing the tumour by limiting its blood supply will also limit its lethality.

The study of angiogenesis is not only carried out in labs, but mathematical modelling can help in getting a deeper understanding of the mechanisms behind it, in the economical and rigorous environment of mathematics. It is outstanding that such a simplification of angiogenesis, despite the complexity of the process, can lead to very realistic results. Chapter 3 investigates the construction and results of three key models in the literature of mathematical modelling of angiogenesis, clearly showing how results from earlier models justify assumptions of later ones.

Chaplain and Stuart developed one of the first one-dimensional continuum models of the process, highlighting the role of proliferation and migration of endothelial cells in it [4]. Initially migration occurs in the direction of the tumour, as the cells go up the gradient of TAF concentration, while proliferation starts later and is confined in a region behind the sprout tips. They are separate steps of angiogenesis, both essential for its completion. Moreover, the TAF concentration profile is such that it would not be unreasonable to assume it to be linear across the domain for the whole duration of vessel formation. This assumption was used by Orme and Chaplain as they developed the first two-dimensional continuum model of tumour-induced angiogenesis, studying not only chemotaxis but also haptotaxis as key mechanisms in the process [5]. While chemotaxis determines the migration of the sprouts towards the tumour, haptotaxis is responsible for lateral movement – together with

random motion of cells – leading to branching and anastomosis, overall determining the completion of a well structured vascular network in which blood can flow. The authors also showed that simple parameter modification allows for simulations of anti-angiogenesis therapy. Finally, Anderson and Chaplain’s two dimensional model for sprout tips cells confirmed the role of haptotaxis in the process, while exploring different tumour geometries [6]. This demonstrated that mathematical modelling has the potential for comparison with both *in vitro* and *in vivo* experiments. Moreover, the derivation of a cellular automaton model from the corresponding continuum one presented by Anderson and Chaplain in 1998 lead to the start of a whole new class of hybrid models, known as snail trail models.

Since 1985, also thanks to the models mentioned above, academic literature has witnessed the expansion of this field of study with new models and investigations proposed, leaning towards a more theoretical approach in one direction and towards the clinic in another. There are still many unanswered questions in the study of cancer and, in particular, angiogenesis, as well as many more mathematical tools to be used in models. Discrete models and implementation of blood flow can be of great use in the study and monitoring of drug delivery through the circulatory system. This field of study has the potential for further expansion in academic research, as well as the potential to get closer to patients. Professor Mark Chaplain’s academic ultimate goal is to develop a virtual tumour [18]: this would allow biologists and medics to quickly simulate growth scenarios as well as treatments. The history and progress of models of tumours suggests that such goal is indeed achievable, although it is hard to say how long this will take, due to the complex nature of cancer. Overall it is clear that mathematical modelling of tumour-induced angiogenesis is a fascinating area of scientific research, with already an active role in the battle against cancer.

Bibliography

- [1] H. M. Byrne. Dissecting cancer through mathematics: from the cell to the animal model. *Nature Reviews Cancer*, 10:221–230, Mar 2010. doi:10.1038/nrc2808.
- [2] K. J. Pienta and J. Zarif. Introduction to the Biology of Cancer by Johns Hopkins University, 2017. Online course on Coursera, available at <https://www.coursera.org/learn/cancer/home/welcome>, completed on June 12, 2017.
- [3] R. A. Weinberg. *The biology of Cancer*. Garland Science, Taylor & Francis Group, 711 Third Avenue, New York, NY 10017, USA, and Park Square, Milton Park, Abingdon, OX144RN, UK, 2nd edition, May 2013.
- [4] M. A. J. Chaplain and A. M. Stuart. A model mechanism for the chemotactic response of endothelial cells to tumour angiogenesis factor. *IMA Journal of Mathematics Applied in Medicine & Biology*, 10(3):149–168, Sep 1993.
- [5] M. E. Orme and M. A. J. Chaplain. Two-dimensional models of tumour angiogenesis and anti-angiogenesis strategies. *IMA Journal of Mathematics Applied in Medicine & Biology*, 14(3):189–205, Sep 1997.
- [6] A. R. A. Anderson and M. A. J. Chaplain. Continuous and discrete mathematical models of tumour-induced angiogenesis. *Bulletin of Mathematical Biology*, 60(5):857900, Sep 1998.
- [7] OpenStax. *Anatomy and Physiology*. OpenStax, Feb 2016. Chapter 20.1 Structure and Function of Blood Vessels, Online at <https://opentextbc.ca/anatomyandphysiology/chapter/20-1-structure-and-function-of-blood-vessels/>, last accessed 30/03/2018.
- [8] The Franklin Institute. The Heart: The Engine of Life, 2018. Section: Blood Vessels. Online at <https://www.fi.edu/heart/blood-vessels>, last accessed 30/03/2018.
- [9] T. H. Adair and J. P. Montani. *Angiogenesis*. Morgan & Claypool Life Sciences, San Rafael (CA), 1st edition, 2010. Online at <https://www.ncbi.nlm.nih.gov/books/NBK53242/>.
- [10] F. Donate. Antiangiogenic therapy in cancer. *Drugs of the Future*, 30(7):695–707, Jul 2005. Table 1: Pro-angiogenic factors. DOI: 10.1358/dof.2005.030.07.929861.
- [11] D. A. de Souza Junior, A. C. Borges, A. C. Santana, C. Oliver, and M. C. Jamur. Mast Cell Proteases 6 and 7 Stimulate Angiogenesis by Inducing Endothelial Cells to Release Angiogenic Factors. *PloS one*, 10:e0144081, 12 2015. Table 2. Action of differentially released angiogenic factors.

- [12] G. Breier. Angiogenesis in Embryonic Development - A Review. *Placenta*, 21:S11–S15, Mar 2000. Supplement A. Available online at https://ac.els-cdn.com/S0143400499905258/1-s2.0-S0143400499905258-main.pdf?_tid=9011028b-23ec-4f15-b4b2-b19e3f42b536&acdnat=1522922014_2243961c4ae9b83694e1b8abe82a345e.
- [13] P. E. Simon. Skin Wound Healing. *Medscape*, Jan 2016. Online at <https://emedicine.medscape.com/article/884594-overview>.
- [14] V. R. Muthukaruppan, L. Kubai, and R. Auerbach. Tumor-induced neovascularization in the mouse eye. *JNCI: Journal of the National Cancer Institute*, 69(3):699–708, Sep 1982. Available online at <https://doi.org/10.1093/jnci/69.3.699>.
- [15] D. Balding and D. L. S. McElwain. A mathematical model of tumour-induced capillary growth. *Journal of Theoretical Biology*, 114(1):53–73, May 1985. Available online at [https://doi.org/10.1016/S0022-5193\(85\)80255-1](https://doi.org/10.1016/S0022-5193(85)80255-1).
- [16] C. L. Stokes and D. A. Lauffenburger. Analysis of the roles of microvessel endothelial cell random motility and chemotaxis in angiogenesis. *Journal of Theoretical Biology*, 152(3):377–403, Oct 1991. Available online at [https://doi.org/10.1016/S0022-5193\(05\)80201-2](https://doi.org/10.1016/S0022-5193(05)80201-2).
- [17] M. M. Sholley, G. P. Ferguson, H. R. Seibel, J. L. Montour, and J. D. Wilson. Mechanisms of neovascularization. Vascular sprouting can occur without proliferation of endothelial cells. *Lab Invest.*, 51(6):624–634, Dec 1984.
- [18] M. A. J. Chaplain. Mathematical modelling, mutations and metastases: can we cure cancer with calculus? Inaugural lecture, 11 April 2018, School III, St Salvator’s Quad, St Andrews (UK).
- [19] COMSOL Multiphysics Modeling Software. <https://www.comsol.com/>. Last accessed: 07/04/2018.

Appendix A

Nondimensionalisation

Nondimensionalisation of the model of Chaplain & Stuart (1992)

Here are the steps of the nondimensionalisation of the model of Chaplain & Stuart (1993) [4] presented in chapter 3.2. The nondimensionalisation of the model of Orme & Chaplain (1997) [5] in section 3.3.1 and of the model of Anderson and Chaplain (1998) [6] in section 3.3.2 can be derived in a similar way.

Define the new rescaled variables as: $\tilde{c} = c/c_b$, $\tilde{n} = n/n_0$, $\tilde{x} = x/L$, $\tilde{t} = t/\tau$.

Then, by chain rule, the differential operators become:

$$\begin{aligned}\frac{\partial}{\partial t} &= \frac{\partial}{\partial \tilde{t}} \cdot \frac{\partial \tilde{t}}{\partial t} = \frac{\partial}{\partial \tilde{t}} \cdot \frac{1}{\tau} = \frac{1}{\tau} \frac{\partial}{\partial \tilde{t}}; \\ \frac{\partial}{\partial x} &= \frac{\partial}{\partial \tilde{x}} \cdot \frac{\partial \tilde{x}}{\partial x} = \frac{\partial}{\partial \tilde{x}} \cdot \frac{1}{L} = \frac{1}{L} \frac{\partial}{\partial \tilde{x}}; \\ \frac{\partial^2}{\partial x^2} &= \frac{\partial}{\partial x} \left(\frac{\partial}{\partial x} \right) = \frac{1}{L} \frac{\partial}{\partial \tilde{x}} \left(\frac{1}{L} \frac{\partial}{\partial \tilde{x}} \right) = \frac{1}{L^2} \frac{\partial^2}{\partial \tilde{x}^2}.\end{aligned}$$

Then equation (3.1) in 1D becomes

$$\begin{aligned}\frac{\partial c}{\partial t} &= D_c \nabla^2 c - \frac{Q_c c n}{(K_m + c)n_0} - dc, \\ \frac{1}{\tau} \frac{\partial}{\partial \tilde{t}}(c_b \tilde{c}) &= D_c \frac{1}{L^2} \frac{\partial^2}{\partial \tilde{x}^2}(c_b \tilde{c}) - \frac{Q_c c_b \tilde{c} p \sigma \tilde{n}}{(K_m + c_b \tilde{c}) p \sigma} - d c_b \tilde{c}, \\ \frac{\partial \tilde{c}}{\partial \tilde{t}} &= \frac{\tau}{\cancel{\sigma}} \frac{D_c \cancel{\sigma}}{L^2} \frac{\partial^2 \tilde{c}}{\partial \tilde{x}^2} - \frac{\tau}{\cancel{\sigma}} \frac{Q_c \cancel{\sigma} \tilde{c} \tilde{n}}{(K_m + c_b \tilde{c})} - \frac{\tau}{\cancel{\sigma}} d \cancel{\sigma} \tilde{c}, \\ \frac{\partial \tilde{c}}{\partial \tilde{t}} &= \frac{\partial^2 \tilde{c}}{\partial \tilde{x}^2} - \frac{Q_c L^2}{D_c} \frac{\tilde{c} \tilde{n}}{c_b \left(\frac{k_m}{c_b} + \tilde{c} \right)} - \frac{d L^2}{D_c} \tilde{c}, \quad \text{for } \tau = \frac{L^2}{D_c};\end{aligned}$$

by setting $\alpha = \frac{L^2 Q}{D_c c_b}$, $\gamma = \frac{K_m}{c_b}$, $\lambda = \frac{L^2 d}{D_c}$, the new nondimensional equation becomes:

$$\frac{\partial \tilde{c}}{\partial \tilde{t}} = \frac{\partial^2 \tilde{c}}{\partial \tilde{x}^2} - \frac{\alpha \tilde{c} \tilde{n}}{(\gamma + \tilde{c})} - \lambda \tilde{c}, \tag{A.1}$$

which, by dropping the tildes for convenience, gives equation (3.9).

Similarly, equation (3.4) in 1D becomes:

$$\begin{aligned}\frac{\partial n}{\partial t} &= D_n \nabla^2 n - \chi_0 \nabla \cdot (n \nabla c) + rn \left(1 - \frac{n}{n_0}\right) G(c) - k_p n, \\ \frac{1}{\tau} \frac{\partial}{\partial \tilde{t}} (n_0 \tilde{n}) &= D_n \frac{1}{L^2} \frac{\partial^2}{\partial \tilde{x}^2} (n_0 \tilde{n}) - \chi_0 \frac{1}{L} \frac{\partial}{\partial \tilde{x}} \left(n_0 \tilde{n} \frac{1}{L} \frac{\partial}{\partial \tilde{x}} (c_b \tilde{c})\right) + rn_0 \tilde{n} \left(1 - \frac{n_0 \tilde{n}}{p\sigma}\right) G(c_0 \tilde{c}) - k_p n_0 \tilde{n}, \\ \frac{\partial \tilde{n}}{\partial \tilde{t}} &= \frac{\tau}{p\sigma} \frac{D_n p\sigma}{L^2} \frac{\partial^2 \tilde{n}}{\partial \tilde{x}^2} - \frac{\tau}{p\sigma} \frac{\chi_0 p\sigma c_b}{L^2} \frac{\partial}{\partial \tilde{x}} \left(\tilde{n} \frac{\partial \tilde{c}}{\partial \tilde{x}}\right) + \frac{\tau}{p\sigma} r p\sigma \tilde{n} (1 - \tilde{n}) G(\tilde{c}) - \frac{\tau}{p\sigma} k_p n_0 \tilde{n}, \\ \frac{\partial \tilde{n}}{\partial \tilde{t}} &= \frac{D_n}{D_c} \frac{\partial^2 \tilde{n}}{\partial \tilde{x}^2} - \frac{\chi_0 c_b}{D_c} \frac{\partial}{\partial \tilde{x}} \left(\tilde{n} \frac{\partial \tilde{c}}{\partial \tilde{x}}\right) + \frac{r L^2}{D_c} \tilde{n} (1 - \tilde{n}) G(\tilde{c}) - \frac{k_p L^2}{D_c} \tilde{n}, \quad \text{for } \tau = \frac{L^2}{D_c}.\end{aligned}$$

By setting $D = \frac{D_n}{D_c}$, $\kappa = \frac{c_b \chi_0}{D_c}$, $\mu = \frac{L^2 r}{D_c}$, $\beta = \frac{L^2 k_p}{D_c}$, the new nondimensional equation becomes:

$$\frac{\partial \tilde{n}}{\partial \tilde{t}} = D \frac{\partial^2 \tilde{n}}{\partial \tilde{x}^2} - \kappa \frac{\partial}{\partial \tilde{x}} \left(\tilde{n} \frac{\partial \tilde{c}}{\partial \tilde{x}}\right) + \mu \tilde{n} (1 - \tilde{n}) G(\tilde{c}) - \beta \tilde{n}, \quad (\text{A.2})$$

where $G(\tilde{c})$ is the nondimensional version of $G(c)$ derived from (3.5) as follows:

$$G(c) = G(c_b \tilde{c}) = \begin{cases} 0 & \text{if } c_b \tilde{c} \leq c_b \tilde{c}^*, \\ \frac{c_b \tilde{c} - c_b \tilde{c}^*}{c_b} & \text{if } c_b \tilde{c} > c_b \tilde{c}^*, \end{cases} = \begin{cases} 0 & \text{if } \tilde{c} \leq \tilde{c}^*, \\ \tilde{c} - \tilde{c}^* & \text{if } \tilde{c} > \tilde{c}^*. \end{cases} \quad (\text{A.3})$$

By dropping the tildes for simplicity, these correspond to equations (3.10) and (3.11).

Initial conditions on \tilde{n} are straightforward from (3.6):

$$\tilde{n}(\tilde{x}, 0) = \frac{1}{n_0} n(x/L, 0) = \begin{cases} \frac{1}{n_0} n_0 & \text{if } x = L, \\ \frac{1}{n_0} \cdot 0 & \text{if } x < L, \end{cases} = \begin{cases} 1 & \text{if } \tilde{x} = 1, \\ 0 & \text{if } \tilde{x} < 1. \end{cases} \quad (\text{A.4})$$

The zero-flux boundary conditions remain unchanged, while the Dirichlet boundary condition (3.7) becomes

$$\tilde{n}(\tilde{x} = 1, t) = \frac{1}{n_0} n(x = \tilde{x} \cdot L = L, t) = \frac{1}{n_0} \cdot n_0 = 1. \quad (\text{A.5})$$

In an analogous way, boundary and initial conditions on \tilde{c} can be derived quite straightforwardly. Equation (3.2) depends on $c_0(x)$, which has directly been defined for the nondimensional model for the numerical simulations, while equation (3.3) gives:

$$\tilde{c}(\tilde{x} = 0, t) = \frac{1}{c_b} \cdot c(x = 0, t) = \frac{1}{c_b} \cdot c_b = 1, \quad (\text{A.6})$$

$$\tilde{c}(\tilde{x} = 1, t) = \frac{1}{c_b} \cdot c(x = \tilde{x} \cdot L = L, t) = \frac{1}{c_b} \cdot 0 = 0. \quad (\text{A.7})$$

Nondimensionalisation of the other models presented, by Orme and Chaplain [5] and Anderson and Chaplain [6], follow the same steps presented above.

Appendix B

Numerical simulations

B.1 Matlab code for solution to Chaplain&Stuart model

```
1 clc
2 clear all
3 close all
4
5 %%MT5999 - code1 (Chaplain&Stuart1992)
6
7 nx=200;
8 x=linspace(0,1,nx); %Space discretisation
9 dt=0.05;
10 t=0:dt:0.7; %time discretisation
11 tsolve=[0,0.1,0.3,0.5,0.7]; %Times at which we solve the system
12 m=0; %slab symmetry
13
14 sol = pdepe(m,@pdefun,@icfun,@bcfun,x,tsolve);
15
16 figure; hold on
17 a1 = plot(x,sol(1,:,:1)); M1 = 't=0';
18 a2 = plot(x,sol(2,:,:1)); M2 = 't=0.1';
19 a3 = plot(x,sol(3,:,:1)); M3 = 't=0.3';
20 a4 = plot(x,sol(4,:,:1)); M4 = 't=0.5';
21 a5 = plot(x,sol(5,:,:1)); M5 = 't=0.7';
22 xlabel(['Distance from tumour']);
23 ylabel(['TAF concentration']);
24 legend([a1;a2;a3;a4;a5], M1, M2, M3, M4, M5);
25
26 figure; hold on
27 b1 = plot(x,sol(1,:,:2)); N1 = 't=0';
28 b2 = plot(x,sol(2,:,:2)); N2 = 't=0.1';
29 b3 = plot(x,sol(3,:,:2)); N3 = 't=0.3';
30 b4 = plot(x,sol(4,:,:2)); N4 = 't=0.5';
```

```

31 | b5 = plot(x,sol(5,:,:2)); N5 = 't=0.7';
32 | xlabel(['Distance from tumour']);
33 | ylabel(['Endothelial cell density']);
34 | legend([b1;b2;b3;b4;b5], N1, N2, N3, N4, N5);
35 |
36 %_____
37 function [c,f,s] = pdefun(x,t,u,DuDx)
38 %parameters
39 alpha=10;
40 gamma=1;
41 lambda=1;
42 d=10^(-3);
43 k=0.75;
44 nu=100;
45 beta=4;
46 cs=0.2; %c*
47
48 c=[1;1];
49 f=[DuDx(1);d*DuDx(2)-k*u(2)*DuDx(1)];
50 if u(1)>cs
51     g=u(1)-cs;
52 else
53     g=0;
54 end
55 s=[-alpha*u(1)*u(2)/(gamma+u(1))-lambda*u(2);nu*u(2)*(1-u(2))*g-beta*u(2)]
56 end
57 %_____
58 function u0 = icfun(x)
59 n0=x*0;
60 % n0(200)=1;
61 c0=cos(pi*x/2);
62 u0=[c0;n0];
63 end
64 %
65 function [pl,ql,pr,qr] = bcfun(xl,ul,xr,ur,t)
66 pl=[ul(1)-1;0]; %c=1 at x=0
67 ql=[0;1]; %zero flux at x=0
68 pr=[ur(1);ur(2)-1] %c=0 & n=1 at x=1
69 qr=[0;0];
70 end

```

B.2 COMSOL

COMSOL Multiphysics is a simulation software environment for a wide range of applications, including solutions to systems of PDEs at different times in a two-dimensional domain, as needed for this project. It does not require the user to code up the algorithm to solve the system of PDEs, but does it automatically once all information about the problem has been given.

Information needs to be given on the spatial dimension and interface, which includes many physical applications as well as mathematical ones (e.g. PDEs). The type of study also needs to be specified (e.g. time dependent), followed by details on the geometry of the domain, parameter values and variables. In the case of a PDEs solver interface, one would need to specify the coefficients of the different terms in the system of PDEs, as well as boundary conditions and initial conditions. The next step would be deciding how refined the mesh should be. Then the study can be conducted and the results can be visualised in plots or animations and many more useful tool are available.

The files created for the simulation results in this document can be found online at http://www.mcs.st-and.ac.uk/~majc/COMSOL_Code_Angiogenesis_Models/, which may also be reached from Professor Mark Chaplain's webpage <http://www.mcs.st-and.ac.uk/~majc/>, under "COMSOL Code for Angiogenesis Models" at the bottom of the page. The name of each file indicates the authors of the model simulated in the file – either Orme & Chaplain (1997) or Anderson & Chaplain (1998).

COMSOL uses the finite element method to solve PDEs, related to the weak form of solutions of differential equations. In this method, the spatial domain is discretised – with the formation of a mesh – and in each finite element an approximation of the PDEs is derived and solved. To do so, at each time-step COMSOL expresses the approximation to the solution of a PDE – say, $n(x, y)$ – as a linear combination of basis functions. One can decide the nature of such basis functions. In this project the basis functions used are Lagrange quadratic elements, as for default in COMSOL. Such an approximation may take the form

$$n(x, y) = \sum_{i=0}^2 \sum_{j=0}^2 a_{ij} x^i y^j = a_{00} + a_{10}x + a_{01}y + a_{11}xy + a_{20}x^2 + a_{02}y^2 + a_{21}x^2y + a_{12}xy^2 + a_{22}x^2y^2$$

where a_{ij} $i, j = 0, 1, 2$ are unknown constant coefficients to be determined. To determine them in the finite element method, a number of test functions are used. Both sides of the PDE are multiplied by a test function and integrated over the domain. The choice of test functions is also flexible and they can be chosen so that the resulting equations at this step may be simplified in each finite element of the domain, created by the mesh. At the boundaries of each finite element the solution is defined so that it is continuous across the whole domain. At this point we get a system of algebraic equations to be solved to get the coefficients a_{ij} $i, j = 0, 1, 2$. In particular, if we have m unknowns, we may use m test functions to express the system in terms of an $m \times m$ matrix. Then we get an approximate solution to the PDE across the domain. The more refined the mesh, the closer the approximation will be to the actual solution. To iterate over time, COMSOL uses as default the backward Euler time-stepping method, based on finite difference approximations.

More details on the finite element method can be found on the COMSOL website [19], under the multiphysics CYCLOPEDIA section.

Glossary

acidosis: pathologic condition consisting of the accumulation of acid in the body fluids or tissues. 4

adipocytes: cells storing fat, which are part of the connective tissue. 6

adjunctive therapies: secondary treatments used in combination with primary treatment, to enhance it. 13

anaerobic respiration: a form of respiration during which there is no consumption of oxygen. 4

apoptosis: programmed cell death. 4, 12

chemokines: family of cytokines which are chemokinetic and chemotactic, stimulating movement and attraction of leukocytes. 9

clinical trials: investigation of new drugs and treatment methods for cancer, through carefully regulated and monitored patient studies. 13

collagen fiber: fiber varying in diameter from less than $1 \mu\text{m}$ to about $12 \mu\text{m}$, composed of fibrils; it is the main element of irregular connective tissue and others. 13

collagenase: enzyme that catalyzes collagen degradation. 9

connective tissue: tissue characterized by a highly vascular matrix; includes collagenous, elastic, and reticular fibers, adipose tissue, cartilage, and bone; it forms the supporting and connecting structures of the body. 4, 6, 10

cytokines: chemicals secreted by cells to stimulate or inhibit other cells' function; cytokines stimulating growth are called "growth factors". 9, 10

cytotoxic: having a toxic effect on cells. 13

de novo: latin for "from the beginning", "new". 5

diabetic retinopathy: retinal changes in diabetes mellitus, sometimes marked by neovascularization. 5

duodenal ulcer: local excavation of the surface of the duodenum, the first portion of the small intestine. 5

ECM: extracellular matrix; aggregate of proteins secreted by the cells, in which the cells themselves are embedded. 6, 13

elastase: enzyme which can catalyze elastic tissue digestion. 9

embryogenesis: formation and growth of an embryo. 5

endothelial cells: cells composing the inner walls of blood vessels. 4

EPCs: endothelial precursor cells or endothelial progenitor cells; cells residing in the bone marrow, which can differentiate to become endothelial cells. 6, 11

fibrin: fibrous protein involved in blood clotting. 9

fibrinogen: protein converted into fibrin during blood clot formation. 9

fibroblast: cell synthesising the ECM and collagen, part of connective tissue. 6, 9

glycolysis: metabolic pathway that converts glucose into pyruvate. 11

hydroxyproline: amino acid, major component of the protein collagen. 11

in vitro: latin for “within the glass”, in an artificial environment outside the living organism. 15, 31

in vivo: latin for “within the living”, in living organisms. 15, 26, 31

inflammatory cells: cells recruited during an inflammation (e.g. macrophages, leukocytes). 6, 9, 10

integrins: family of cell receptors on cell membrane that promote cell adhesion to the ECM or other cells or others (platelets, fibrinogen, fibronectin). 7, 13

interstitial tissue: connective and supporting tissue both inside and surrounding major functional elements of an organ. 13

intravasation: entry of foreign material in a blood vessel. 13

intussusceptive angiogenesis: process during which an existing blood vessel is split in two, also known as splitting angiogenesis. 5

lactate: a salt or base of lactic acid. 4

lymphocytes: specialised white cells responsible for the body's immune system. 6

macrophages: white blood cells protecting the body from infection and foreign matter. 6, 9, 11

mesenchymal cells: cells in the connective tissue with much greater motility than endothelial cells. 6

mitogenic growth factor: growth factors stimulating mitosis, i.e. cell proliferation. 6, 11

mitosis: cell division process resulting in the formation of two daughter cells. 6

monoclonal antibodies: molecules which synthesise antigens as immune response, produced by myelomas (tumours). 13

myofibroblast: fibroblast with structural features of a smooth muscle cell. 6, 10, 12

necrotic: indicating dead cells or tissues. 4, 10

neoplastic: related to a neoplasm, i.e. a tumour. 10, 12

p53: protein regulating cell growth and proliferation; tumor suppressor gene. 4, 12

parenchymal cells: cells of a gland or organ, part of the connective tissue. 6, 7, 12

pathological process: process involved in some disease. 5

pericytes: mesenchymal cells forming the walls of capillaries. 4, 6, 7, 12

physiological process: process in systems, organs and tissues of organisms. 5

platelets: structures in blood stimulating clotting, shaped like a disk. 9

protease: enzymes that catalyze proteins' break down. 6

psoriasis: skin disease causing red spots covered with silvery scales. 5

receptor: molecular structure either inside or on the surface of a cell that binds with various substances (e.g. hormones, angiogenic factors). 6, 13

rheumatoid arthritis: disease of the musculoskeletal system, causing inflammation of joints, muscle weakness, tiredness. 5

smooth muscle cells: spindle-shaped cells forming muscle tissue which contracts involuntarily, composing the walls of internal organs (including blood vessels). 4, 6, 7, 12

stromal cells: cells of the connective tissue of organs, supporting the function of parenchymal cells (e.g. fibroblasts, pericytes). 6, 10–12

transcription factor: protein that regulates the transcription rate of genetic information from DNA to mRNA. 11

trophic factors: proteins favouring neuron development and connection. 6

tyrosine kinase receptor: receptor on cells' surfaces that binds to many growth factors, cytokines and hormones. 6